5-11-2021

In Vitro Analysis of Antioxidant Poly(Propylene Sulfide)-Microspheres for Pretreatment of Inflammatory Cytokine-Induced Chondrocytes to Facilitate Adipose-Drived Stem Cell Therapy

Zachary Alexander Pasternak

IN VITRO ANALYSIS OF ANTIOXIDANT POLY(PROPYLENE SULFIDE)-MICROSPHERES FOR PRETREATMENT OF INFLAMMATORY CYTOKINE-INDUCED CHONDROCYTES TO FACILITATE ADIPOSE-DERIVED STEM CELL THERAPY

by

Zachary Pasternak

A Thesis

Submitted in Partial Fulfillment of the

Requirements for the Degree of

Master of Science

Major: Biomedical Engineering

The University of Memphis

May 2021

This Thesis is dedicated to my mother Alicia Wilson. Without her endless help and support, this achievement would not have been possible.

Thank you!

Abstract

Evidence supports that osteoarthritis (OA) has a chronic low-grade inflammatory state that contributes to the progressive loss of articular cartilage. Reactive oxygen species (ROS) are elevated following injury and mediate inflammation. Cellular therapy using mesenchymal stem cells (MSCs) induce anti-inflammatory and healing responses in native tissue, but efficacy and reproducibility are lacking. Since OA treatments involving MSCs introduce cells into a damaged and inflamed joint, excess oxidative stress could damage these cells reducing their benefit. Cytokine-stimulated chondrocytes treated with hydrogen peroxide scavenging poly-propylene sulfide microspheres (PPS-MS) showed reduced expression of collagenase (MMP-13) with a narrow window of efficacy. Co-culture investigation with MSCs showed no reduction of MMP-13 expression nor increase in expression of anabolic factors like type II collagen. Pretreatment with PPS-MS prior to the addition of MSC therapy did not provide conclusive evidence for improved anabolic to catabolic gene expression ratios over a five-day culturing period.

Table of Contents

Table of Contents

List of Tables

List of Figures

Abbreviations

ACAN	Aggrecan
ADAMTS4	A disintegrin and metalloproteinase with thrombospondin motifs 4
ADSC	Adipose derived stem cell
Akt	Protein Kinase B
AP-1	activating protein-1
COL2A1	type II collagen
DAMP	damage-associated molecular pattern
DMOAD	Disease Modifying Osteoarthritis Drug
ECM	extracellular matrix
H_2O_2	Hydrogen peroxide
IkB	inhibitor of NF-kB
IL-1β	interleukin-1β
JNK	c-Jun NH_2-terminal kinase
K&L	Kellgren and Lawrence
LPS	lipopolysaccharide
MCP-1	Monocyte chemoattractant protein-1
MAPK	mitogen activated protein kinase
MMP-13	matrix metalloproteinase-13
MSC	mesenchymal stem cell
NF-kB	nuclear factor kappa-light-chain-enhancer of activated B cells
Nox4	NADPH oxidase 4
OA	Osteoarthritis

OCL	osteocalcin
PI3K	Phosphatidylinositol 3-kinase
PPS-MS	poly(propylene sulfide)-microsphere
PRR	pattern recognition receptor
RNS	reactive nitrogen species
ROS	reactive oxygen species
TGFβ	transforming growth factor-β
TLR4	toll-like receptor 4
TNFα	tumor necrosis factor α

Introduction

Osteoarthritis (OA) is a painful, debilitating joint disease of which there is no cure, leaving palliative care as the primary treatment until corrective surgery is required. OA progresses with gradual degeneration of the articular cartilage matrix that is often accompanied by synovial inflammation and subchondral bone sclerosis. Focal mechanical stresses can form deep cracks in the cartilage that penetrate to the calcified zone [1,2]. Although OA refers to the loss of cartilage, it is a total joint disease such that surrounding tissues (synovium, menisci, ligaments, subchondral bone, and infrapatellar fat pad) contribute to maintaining a catabolic state [3,4]. The risk factors for OA are complex depending on several influences like age, obesity, genetics, repetitive injury, and anatomical misalignment [5]. Even with surgical options, joint replacements deteriorate over time necessitating replacement and requiring a more complex and invasive revision arthroplasty [6,7]. The most reasonable approach to avoid surgery is early intervention to mitigate the loss of cartilage. Currently, however, there is no available Disease Modifying Osteoarthritis Drug (DMOAD) that is effective nor approved by the Food and Drug Administration (FDA) leaving pain management strategies as the primary method for treatment [8]. Due to the lack of curative therapies, further investigations into the pathogenesis of OA to reveal unknown mechanisms are needed to improve strategies for developing an effective therapy.

Even though a variety of mechanisms are involved in OA pathogenesis, an imbalance in reactive oxygen species and reactive nitrogen species (ROS/RNS) may contribute to OA by propagating and maintaining a low-grade inflammatory state [9,10]. Antioxidant therapies that scavenge ROS/RNS may prove to be effective strategies for

halting the inflammation. One such potential therapeutic is the poly(propylene sulfide)-microsphere which scavenges hydrogen peroxide, hypochlorous acid, and peroxynitrite (to a small degree) [11]. Hydrogen peroxide is a major mediator for pro-inflammatory transcription factors like NF-kB (nuclear factor kappa-light-chain-enhancer of activated B cells) and AP-1 (activating protein-1). Removing excess hydrogen peroxide may abate signaling and prevent propagation of a catabolic environment [12].

In addition to antioxidant treatments, mesenchymal stem cells (MSCs) have been investigated for regenerative medicine applications due to their plastic-like nature and ability to differentiate into a variety of mature cell types. A potential issue with this approach, however, is the low number of cells that engraft at the injection site. Although limited engraftment occurs, treatment has been reported to considerably reduce fibrosis and scarring at injection sites, indicating that MSCs act as anti-inflammatory agents to promote healing [13]. Instead of using stem cells to replace lost tissue, a focus has shifted to their use as an immunomodulatory treatment that can induce repair in damaged tissue by re-establishing a healthy anabolic/catabolic homeostasis [14].

Structural Changes in the Knee Joint and Characterization

The healthy joint is composed of a sheet of glassy, hyaline cartilage found at the articulating surfaces. The extracellular matrix (ECM) is maintained by the resident cell chondrocytes which make up about 1-3% of the volume [15]. The primary function of articular cartilage is to facilitate the sliding action and movement between bones. There are four zones in the articular cartilage. Starting from the outermost surface is the superficial layer which contains type II collagen fibers orientated parallel to the sliding surface. Cells are also tightly squamous or elliptical in appearance. Further down towards

the bone is the transitional or middle layer which has a high abundance of sulfated proteoglycans that are negatively charged to allow adsorption of water allowing for shock absorption. The collagen fibers are randomly aligned, and cells are dispersed throughout this layer in lacunae containing 2-4 chondrocytes which work to support the extracellular matrix. The next lowest layer is the deep zone which is composed of collagen fibers that are perpendicular to the surface and anchored into the subchondral bone. The deepest layer is the calcified zone which serves as the transition between bone and cartilage as it anchors and fixes the cartilage in place. The calcified zone is separated from the deep zone by the tidemark and consists of hypertrophic chondrocytes [16].

Cartilage differs from other tissues in regard to its healing capabilities due to its avascular state. In the early stages of OA, although there is a loss of proteoglycans, cartilage becomes more hydrated and swells in size due to a disrupted collagen matrix that cannot restrain the proteoglycans [17]. Later on, as more proteoglycans are released, permeability increases leading to decreased shock absorption which increases stiffness causing a heightened propensity to deformation and wear [18], During the initial swelling of cartilage, metabolism is elevated as chondrocytes attempt to repair the surrounding matrix increasing proteoglycan synthesis. This increased metabolic rate is accompanied by a hypertrophic-like phenotype in chondrocytes similar to that of the growth plate [19]. For this reason, certain characteristics of OA progression parallel the embryological formation of bone during endochondral ossification [20,21]. Chondrocyte hypertrophy commonly occurs in the cartilage growth plates as they elongate. As chondrocytes undergo hypertrophy, they begin secreting type X collagen (COL10A1), matrix metalloproteinase-13 (MMP-13), vascular endothelial growth factor (VEGF), alkaline

phosphatase (ALP), and osteocalcin (OCL). ALP and OCL act to calcify the surrounding matrix further blocking nutrient exchange. As hypertrophic chondrocytes die, MMP-13 degrades collagen allowing for vasculature to infiltrate the area with the help of VEGF [22]. Other anabolic factors such as transforming growth factor-β (TGFβ) and bone morphogenetic protein-2 (BMP-2) are also elevated in OA patients which could lead to the formation of bone spurs (osteophytes) and induce hypertrophy in neighboring chondrocytes.

Inflammation and ROS Related to OA and PTOA:

Symptoms of severe OA include osteophyte formation, joint space narrowing, increased pain, swollen and effused joints, and subchondral bone deformation. To classify OA, Kellgren and Lawrence (K&L) developed a radiographic scoring system from grade 0 to 4 with severity increasing with number [23,24]. In cases of severe OA, K&L grade 4, synovitis has been reported in over 83% of patients [25]. Released matrix proteins from degradation and wear aggravate synovitis leading to increased $CD68^{+}$ macrophage numbers, cytokine secretion, and synovial thickening [26]. Although synovitis can be observed as a symptom of OA, evidence suggests that biochemical factors related to this symptom exacerbate and amplify OA progression [27,28]. By considering the knee joint at a component level (i.e. synovitis, osteophytes, subchondral bone, ligaments, and menisci), an effective treatment strategy will likely include a multi-faceted approach to remedy the joint as a collective, whole unit.

Injuries to the joint, if severe enough, will lead to cell death (necrosis and/or apoptosis) and fragmentation of matrix proteins such as type II collagen and other proteoglycans [29]. From this damage, cytokines and chemokines are released which

stimulate cells in a paracrine manner to promote more inflammation and attract leukocytes to the injured area. Surrounding cells in the knee that are affected by cytokine release include synovial fibroblasts, macrophages, chondrocytes, osteocytes, and adipocytes. As these cells transition to a pro-inflammatory phenotype, they produce more cytokines, catabolic proteases, and reactive oxygen species (ROS) [30]. Because sub necrotic injuries can also result in cytokine release, damage to the joint does not need to be a one-time traumatic injury (i.e. PTOA) but can often result from repetitive wear and tear over one's lifetime. Mechanical stress can fragment matrix proteins releasing molecules with damage-associated molecular patterns (DAMPs), synonymous with alarmins, that signal through pattern recognition receptors (PRRs) on surrounding cells (chondrocytes, macrophages, synovial fibroblasts, and ligament fibroblasts) to elicit an inflammatory response and increase ROS leading to cell death [31, 32, 33]. Fibronectin fragments, low-molecular weight hyaluronic acid, S100 proteins, and high mobility group box-1 are a few examples of DAMPs/alarmins that signal through various PRRs [34,35]. Pathogen associated molecules like lipopolysaccharide (LPS) recognize PRRs such as toll-like receptor 4 (TLR4) of which some DAMPs/alarmins activate as well. Downstream signaling from TLR-4 increases ROS and activates NF-κB [36, 37, 38].

In multiple cell lines, cytokine stimulation from interleukin-1β (IL-1β) or tumor necrosis factor α (TNFα) leads to terminal activation of nuclear factor kappa-light-chain-enhancer of activated B cells (NF-κB) and activating protein-1 (AP-1). Both TNFα and IL-1β activate NF-κB through the canonical pathway by activating upstream kinases that phosphorylate the inhibitor of NF-κB (IκBα) at serine residues 32 and 36 leading to its subsequent ubiquitination and proteolytic degradation [39]. With IκBα no longer bound

to NF-κB, the dimer (p65 and p50) is free to translocate into the nucleus and transcribe a multitude of genes with κB promoter regions which regulate inflammation, apoptosis, and proliferation [40, 41]. IL-1β and TNFα activate AP-1 through the downstream mitogen activated protein kinase (MAPK) c-Jun NH_2-terminal kinase (JNK). IL-1β activates other MAPKs as well, such as extracellular signal-regulated kinase (ERK) and p38 [42]. JNK is the kinase that phosphorylates c-Jun leading to dimerization with c-Fos to form the transcription factor AP-1 which binds to promoter regions upstream of multiple genes such as collagenase (MMP-1), stromelysin (MMP-3), and c-Jun [43]. Additionally, JNK and p38 are part of a class of MAPKs known as stress activated protein kinases, which are not only activated by extracellular proteins, but also other environmental factors such as UV radiation, hypoxia, heat shock, and osmotic shock [44]. ROS elevation occurs after cytokine stimulation, but the mechanisms underlying activation of NF-κB and AP-1 are not fully understood. Although antioxidant treatments are shown to reduce NF-κB and AP-1 activation following cytokine stimulation, some evidence indicates that ROS mediated activation of the transcription factors may also be independent from cytokine-mediated activation [45].

Direct addition of H_2O_2 to human epithelial cell (A549) cultures led to the transcription of c-jun indicating an activation of JNK and subsequently AP-1. Hydrogen peroxide, however, did not directly activate JNK as observed from the lack of JNK binding to GST-c-Jun-glutathione beads, so it is proposed that an upstream kinase of JNK is the target for H_2O_2 modification [46]. Phosphatidylinositol 3-kinase (PI3K) is sensitive to hydrogen peroxide and may lead to activation of JNK through an intermediate G-protein exchange factor [47]. PI3K is a versatile activator of several pathways, one of

which includes Akt (Protein Kinase B) which is involved in cell survival, cytoskeleton rearrangement, and metabolism to only name a few cell functions. This activation of Akt could likely contribute to both positive and negative effects of hydrogen peroxide on chondrocyte metabolism. Therefore, a balance in ROS is important to maintain so that over scavenging is avoided which can result in cellular dysfunction [48,49]. Additionally, activation of NF-κB by hydrogen peroxide may be achieved through PI3K as well. An alternate pathway for NF-κB was discovered involving the phosphorylation of IκB at tyrosine 42, rather than serine residues 32 and 36. This alternate phosphorylation does not lead to proteolytic degradation of IκB but does cause IκB to dissociate from NF-κB [50].

Even though hydrogen peroxide is an important secondary messenger in oxidative stress, other ROS and RNS have been shown to mediate inflammatory signaling and apoptosis. Increased oxidative stress from ROS/RNS has also been associated with a number of diseases such as diabetes, dementia, and cancer [51]. ROS is an umbrella term that includes both free radicals and non-radical oxygen containing molecules. The free radicals are the most damaging and transient particles, causing protein cleavage and chain breaks along DNA. Free-radicals often break down into other non-radical ROS and oxidize lipids which remain in the microenvironment longer increasing oxidative stress [52]. Of the free-radical ROS, the hydroxyl radical (•OH) is the most reactive and damaging which can be formed from the reduction of hydrogen peroxide (H_2O_2) by iron (Fe^{2+}) [53]. TNFα, IL-1β, and interferon-γ (IFNγ) have been shown to increase ROS/RNS levels by activating and increasing expression of iNOS (inducible nitric oxide synthase). Nitric oxide (NO•) can react with superoxide ($•O_2^-$) to produce peroxynitrite ($ONOO^-$)

which can spontaneously decompose into the hydroxyl radical [54, 55]. Cytokines (TNFα, granulocyte-macrophage colony-stimulating factor, and IL-8) and LPS prime leukocytes such as neutrophils and macrophages to produce a larger respiratory burst which increases ROS to degrade ingested bacteria and cellular debris [56, 57]. Furthermore, macrophages can induce cytotoxicity extracellularly, by non-phagocytic means, through the release of nitric oxide which expels iron from iron-sulfur clusters [4Fe-4S] [58].

Superoxide radicals can be formed from the incomplete reduction of oxygen through NADPH oxidases (NOX) located in the mitochondrial membrane. Superoxide dismutase reduces the superoxide radical to hydrogen peroxide. A study investigating ROS production from cytokine-stimulated mouse chondrocytes determined that the frequency of superoxide generation in mitochondria increased 2-fold within an hour of stimulation. Furthermore, the increase in these superoxide bursts rose to almost 5-fold within 2 hours under continual stimulation from IL-1β [59]. The mechanism as to how cytokines cause increased burst firing of superoxide by the mitochondria is not established. An interesting NOX isotype is Nox4 which does not produce superoxide radicals but rather hydrogen peroxide instead. However, the uniqueness of Nox4 is that it is constitutively active rather than induced, so as expression increases in the cell, it may play a role in chronically elevating ROS levels [60]. In human OA articular chondrocytes, gene expression levels of Nox4 were found to be elevated nearly 14-fold compared to non-OA chondrocytes [61]. Furthermore, treating chondrocytes with IL-1β and TNFα initially lead to a decrease in Nox4 expression, but after 24 hours, levels of

Nox4 were nearly tripled [62]. These elevations in ROS following injury are contributing factors to chronic inflammation and further self-perpetuate the ROS imbalance.

PPS-MS as a Hydrogen Peroxide Scavenger

The polypropylene sulfide-microspheres (PPS-MS) consist of polymer spheres roughly 1μm in diameter. Several studies have shown that these polymer microspheres can scavenge various ROS [63, 64]. Based on scavenging experiments the PPS-MS is mostly reactive with hydrogen peroxide (H_2O_2) and hypochlorite (^-OCl) while being slightly reactive towards peroxynitrite ($ONOO^-$). The microspheres do not scavenge superoxide (O_2^-) and nitrite (NO_2^-). When introduced into an appropriate oxidizing environment, the sulfide (R_2S^{2-}) will react to form a sulfone (R_2SO_2) and solubilize in the process (Figure 1, adapted from O'Grady et al.) [9].

This degradation of the microsphere can be utilized to deliver drugs in an area that has a high concentration of ROS [65]. Additionally, the PPS polymer has been coupled with other polymers (natural and synthetic) for encapsulating stem cells to aid cell-based therapies [66]. In a study that conditioned stem cells with antioxidants (glutathione or melatonin), the investigators found a significant increase liver retention for injected ADSC that was superior to non-conditioned ADSCs. Furthermore, hydrogen peroxide stimulation was shown to increase pro-apoptotic Bax while decreasing anti-apoptotic Bcl-2 and the chemokine receptor type 4 which is reported to mediate stem cell migration and homing. Antioxidant treatment attenuated the changes in these protein levels as well [67]. By reducing ROS in the joint with PPS, ADSC treatment may be sustained longer and more effective. Additionally, the large size of the microspheres allows for longer retention in the injected site compared to nanospheres. The increased size can also be

more susceptible to phagocytosis from resident macrophages which can suppress inflammatory signaling mediated by ROS [8].

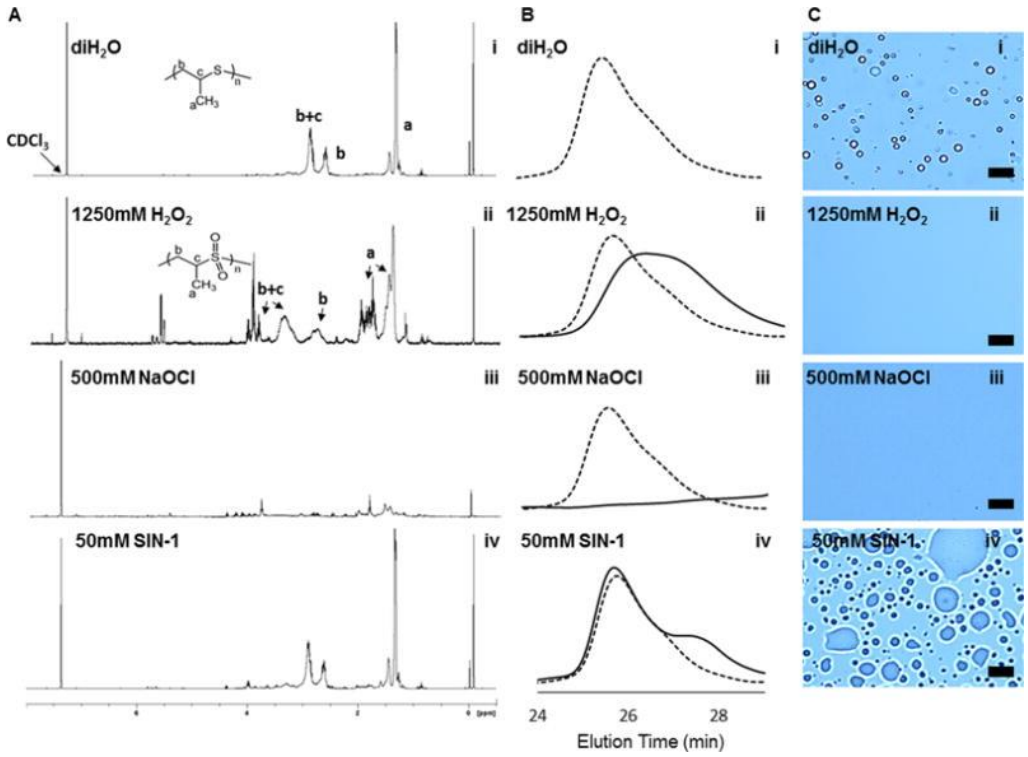

Figure 1: PPS-MS oxidation and subsequent solvation in the presence of hydrogen peroxide and hypochlorous acid (produced by sodium hypochlorite). There is a swelling effect for nitric oxide (produced by SIN-1) but minimal scavenging occurs. In the presence of water, PPS-MS does not dissolve. Adapted from O'Grady et al. and reprinted with permission from American Chemistry Society Biomaterials Science & Engineering [9].

Stem Cells as Anti-Inflammatory Agents

The modern conception of stem cells was originally formulated by Friedenstein *et al*. indicating a cell of mesenchyme origin that has the propensity to differentiate into bone or cartilage [68]. Originally isolated from the bone marrow, mesenchymal stem/stromal cells (MSC) have since been recovered from several other tissues such as

fat, umbilical cord, muscle, and skin [69]. In addition to the capability of differentiating into bone, cartilage, and adipose tissue, surface markers positive for CD90 and CD29 while being negative for CD45 have been used to characterize stem cells [70]. For purposes of cell therapy, adipose-derived stem cells (ADSCs) are the most appropriate because they originate from an abundant source of tissue and are more numerous per volume unit than bone-marrow.

MSCs possess sensing capabilities that seemingly act to maintain a consistent level of inflammatory mediators. When levels of IFNγ and TNFα are high, MSCs respond by secreting IL-6, IDO (Indolamine 2,3-dioxygenase) and PGE2 (Prostaglandin E2) which promotes the emergence of an anti-inflammatory M2 phenotype with increased secretions of IL-6, IL-10, and TGFβ1 [71]. IL-6 presents an interesting case because of its pleiotropic nature leading to a variety of unique and paradoxical effects based on specific cell activation. IL-6 is released in the acute phase response of injury and is the most elevated cytokine detected in synovial aspirates. IL-6 is also known as HSF (hepatocyte stimulating factor) causing liver cells to secrete CRP (C-reactive protein). The role that IL-6 plays in OA is unknown and complex. Activation of the IL-6 receptor leads to downstream phosphorylation and dimerization of STAT3 (signal transduction and activator of transcription 5). If un-phosphorylated, STAT3 can associate with the p65 subunit of NF-κB, so IL-6 activation of its receptor may be necessary for preventing STAT3-p65 association and transcriptional activation [72]. By itself, STAT3 can lead to the transcription of hundreds of genes, so it is no trivial task to determine a pro- or anti-inflammatory status for IL-6.

In the presence of TNFα, MSCs secrete TSG-6 (TNF-stimulated gene 6) which blocks transition of macrophages to an M1 state by inhibiting NF-kB. Not only does TSG-6 block M1 transition but it has also been reported to induce an M2 phenotype in macrophages leading to release of PGE2 and IL-1Ra. In co-culture *in vitro* models combining ADSCs with cytokine (TNFα or IL-1β) stimulated chondrocytes, induced expression of MMP-13 and other cytokines like IL-1β, IL-6, and TNFα are reduced. Additionally, ADSCs appear to secrete a steady amount of TIMPs which can not only inhibit MMPs but other metalloproteinases as well like ADAMTS-4 (A disintegrin and metalloproteinase with thrombospondin motifs 4) [73, 74, 75].

Hypothesis:

Treatment of chondrocytes, that were stimulated with cytokines to induce inflammatory pathways, with hydrogen peroxide scavenging polypropylene-microspheres (PPS-MS) was hypothesized to reduce catabolic gene expression. It was also hypothesized that PPS-MS would attenuate cell death from exogenous hydrogen peroxide. It was further hypothesized that combining both ADSCs and PPS-MS would further reduce catabolic MMP-13 expression.

Methods

Cytokine Stimulated Chondrocytes Treated with PPS-MS

The purpose of performing this experiment was to test the hypothesis that addition of PPS-MS would reduce the catabolic increase of MMP-13 while attenuating the loss of anabolic (ACAN and COL2A1) gene expression from cytokine stimulation. To perform this experiment, $4.0x10^5$ pig chondrocytes (passages 1-3) were plated per well in a 24-well plate. Cells were cultured for 48-hours with media being replenished after the first

24-hours allowing the chondrocytes to form a suitable matrix. The culture media was F12K supplemented with 10% fetal bovine serum (FBS), 40mM ascorbic acid, 2mM L-glutamine, and 1% Penicillin/Streptomycin (P/S). After culturing, chondrocytes were pre-stimulated with PPS-MS at various concentrations (2X of final concentration) for 1hr in 500µL of serum-free culture media. After pre-treatment, 500µL of a 10ng/mL solution containing TNFα or IL-1β in serum-free F12K with 40mM ascorbic acid was added so that the final concentration of the cytokine would be 5ng/mL. RNA was extracted using Trizol reagent 24hrs after cytokine addition. Gene expression was performed for anabolic (COL2A1 and ACAN), catabolic (MMP-13 and ADAMTS4), and inflammatory (MCP-1) genes using the delta Ct method with reverse transcription quantitative real-time polymerase chain reaction (RT-qPCR).

IL-1β Stimulated Chondrocytes Indirectly Co-Cultured with ADSCs

The purpose of performing this experiment was to test the hypothesis that addition of ADSCs would reduce the catabolic increase of MMP-13 while attenuating the loss of anabolic (ACAN and COL2A1) gene expression from cytokine stimulation. To perform this experiment, $4.0x10^5$ pig chondrocytes were plated per well in a 24-well plate. Cells were cultured for 48-hours with media being replenished after the first 24-hours allowing the chondrocytes to form a suitable matrix. The culture media contained F12K + 10%FBS + 40mM ascorbic acid + 1% Penicillin/Streptomycin + 2mML-glutamine. After culturing, chondrocytes were stimulated with IL-1β (5ng/mL) for 24hrs in serum-free F12k containing 40mM ascorbic acid. After the stimulation period, chondrocytes were washed with phosphate buffered saline (PBS), and $2.5x10^4$ ADSCs were added indirectly (via transwell inserts) in 10%FBS F12K with 40mM ascorbic acid with or without

2.5µg/mL of PPS-MS. RNA was extracted using Trizol reagent 24hrs after cytokine addition. Gene expression was performed for anabolic (COL2A1 and ACAN) and catabolic (MMP-13) genes using the delta Ct method with qPCR.

Oxidative Stress Impact on ADSCs with PPS-MS Treatment

The purpose of performing this experiment was to test the hypothesis that PPS-MS would alleviate potential damaging effects of oxidative stress that might induce cell death of ADSCs. To start this experiment, a dose response for hydrogen peroxide to determine a concentration that would lead to 50% death (LD_{50}) within 24-hours after initial stimulus was performed. Initially, $5.0x10^3$ ADSCs were plated with reduced FBS media (HG-DMEM with 2% fetal bovine serum (FBS), 2mM L-glutamine, and 1%Penicillin/Streptomycin) supplemented with various concentrations of hydrogen peroxide. Using CellTiter-Glo to measure luminescence of ATP, indicating viability, a LD_{50} concentration of hydrogen peroxide was determined. Using the established LD_{50} concentration, a follow-up experiment was performed to measure viability of ADSCs at various concentrations of PPS-MS 24-hours after initial dose of the LD_{50} hydrogen peroxide concentration. Another LD_{50} study was performed to determine the effect that cell number has on the LD_{50}. For this experiment, $5.0x10^3$ ADSCs or $1.0x10^4$ ADSCs were plated per well in a 96-well with reduced FBS media (HG-DMEM with 2% fetal bovine serum (FBS), 2mM L-glutamine, and 1% Penicillin/Streptomycin) supplemented with various concentrations of hydrogen peroxide). CellTiter-Glo assay was performed again to determine viability of ADSCs after exposure to hydrogen peroxide.

Chondrocytes Pretreated with PPS-MS then co-cultured with ADSCs for 5 days

This experiment is the final experimental method compiled from the previous experiments. The goal of this experiment was to test the hypothesis for any additive or synergistic results that PPS-MS and ADSCs could achieve for anti-inflammatory effects on cytokine-treated (damaged) chondrocytes. The experimental setup was designed to mimic an injury that received an antioxidative treatment to reduce inflammation prior to a stem cell injection. $4.0x10^5$ chondrocytes were seeded per well in a 24-well plate and allowed to adhere overnight in F12k + 10% FBS + 40mM ascorbic acid + 1% penicillin/streptomycin + 2mM L-Glutamine. Media was replenished the next day to allow chondrocytes to produce matrix. Chondrocytes were stimulated with cytokine (IL-1β at 5ng/mL) in serum-free F12k without ascorbic acid to prevent additive antioxidant effects separate from those of PPS-MS. After 4hours of cytokine stimulation, media was supplemented with 2.5µg/mL of PPS-MS. After 20 hours, stimulation media was removed, cells were washed with PBS and co-cultured in the presence or absence of $3.5x10^4$ ADSCs in transwell inserts. RNA was extracted at the end of the stimulation period (day 0) and 5 days after co-culturing began. Fresh media was changed every two days.

Reverse Transcription Quantitative Real-Time PCR (RT-qPCR)

Gene expression via is calculated by finding the cycle threshold (Ct) of a gene's measured fluorescence which is emitted by a specific binding primer to the gene of interest (GOI). The GOI Ct value is then subtracted from the Ct value of a housekeeping gene (also known as a reference gene) which should not change given the experimental conditions – this is the ΔCt value [76]. Each sample ΔCt value is then subtracted from the

average of the control ΔCt value to give the ΔΔCt value. Finally, it is converted to a log2 scale because each cycle number represents a doubling that occurs during the polymerase chain reaction. The lower Ct value for a GOI that is found the more numerous that gene is. Ct values above 30 have low expression, with values found above 35 expected to be a false positive from non-specific primer binding. The importance of normalizing to a housekeeping gene is to avoid any errors in quantifying GOI due to RNA extraction, pipetting errors, or inequalities in enzyme activity during the reverse-transcription polymerase chain reaction (RT-PCR) [77]. TaqMan® probes (i.e. hydrolysis probes) were used to target COL2A1, ACAN, MMP-13, ADAMTS4, MCP-1, Nox4, and GAPDH.

Statistical Analysis

Statistical analysis for data were performed in Sigma Plot. Normality was checked using Shapiro-Wilk, equal variances were checked using Brown-Forsythe. Data meeting normality and equal variance assumptions were analyzed using one-way ANOVA with Holm-Sidak corrections. For comparisons between two groups, Student's t-test was used if normality and equal variance were assumed. Nonparametric Kruskal Wallis ANOVA analyses with Tukey post hoc corrections were performed if normality and equal variance requirements were not met. Nonparametric t-tests (Welch's method) with Bonferroni corrections were also used if equal variance was not met. Significance, alpha, was set at 0.05 with n = 3 samples for most groups.

Results

Cytokine Stimulated Chondrocytes Treated with PPS-MS

Gene expressions shown for TNFα-stimulated chondrocytes include MMP-13, ACAN, and COL2A1 were measured in this experiment using the 2^-ΔΔCt method normalized to the housekeeping gene GAPDH. In this experiment, the addition of TNFα (5ng/mL) increased catabolic MMP-13 expression. TNFα stimulation also led to a drop in the anabolic gene expressions COL2A1 and ACAN; there was no recovery in anabolic expressions with PPS-MS treatment (Figures 2 and 3). PPS-MS at a concentration of 2.5μg/mL and 5.05μg/mL resulted in significantly lower MMP-13 expressions $p = 0.006$ and $p=0.022$, respectively (Figure 4).

Gene expression shown for IL-1β stimulated chondrocytes include ADAMTS4 and MCP-1. Stimulating chondrocytes with IL-1β (5ng/mL) leads to an increase in ADAMTS4 and MCP-1 gene expressions (Figures 5 and 6). PPS-MS treatment at 5μg/mL significantly reduced ADAMTS4 expression from stimulated chondrocytes with a p-value = 0.022 (Figure 5). MCP-1 expressions were reduced using PPS-MS at a concentration of 0.625μg/mL with p-value = 0.08 (Figure 6). Due to the high amount of variation in MCP-1 gene expression for unstimulated control the average 2^-ΔΔCt value is not equal to 1.00 (Table 5). In unstimulated chondrocytes, addition of PPS-MS did not have any significant effect on gene expression (Figure 7).

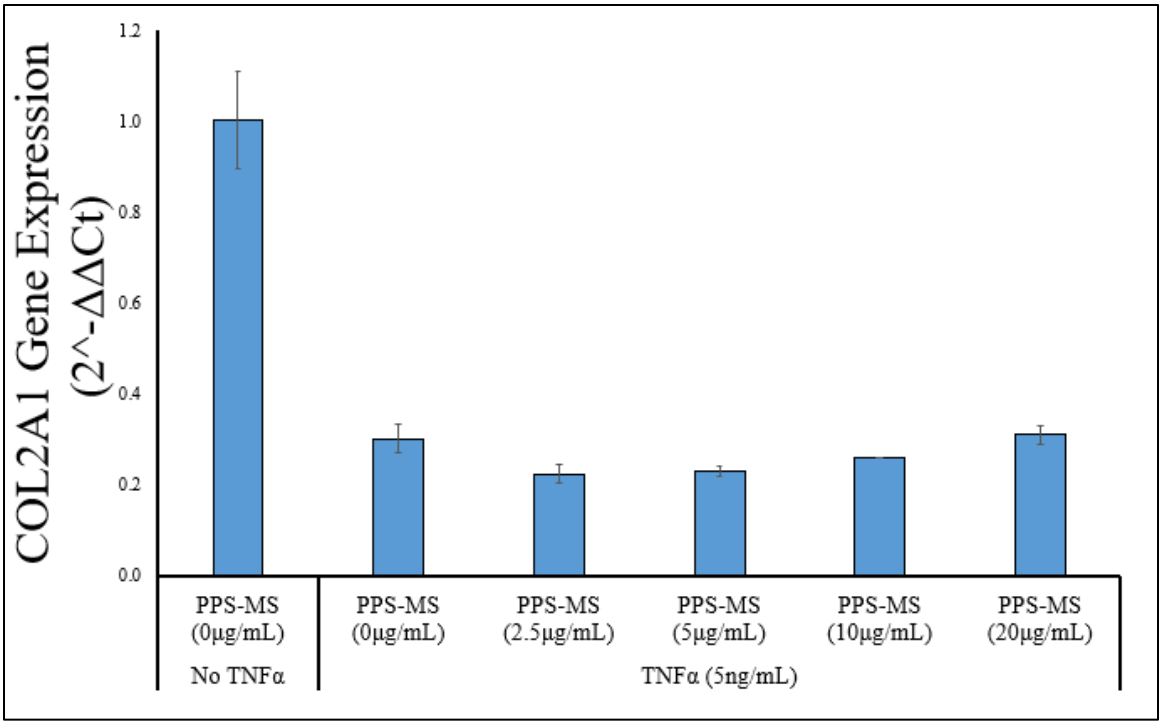

Figure 2: Graph shows COL2A1 gene expression for chondrocytes stimulated with TNFα normalized to GAPDH. n = 3 for most groups; n = 2 for TNFα (5ng/mL) + PPS-MS (2.5µg/mL); n = 1 for TNFα (5ng/mL) + PPS-MS (10µg/mL). All cells stimulated with TNFα were significantly different from control ($p < 0.001$). No significant differences were detected between TNFα stimulated cells treated with PPS-MS and non-treated cells. Bars represent mean and error bars represent standard deviation. One-way ANOVA with Holm-Sidak corrections were used to determine significance.

Table 1: Corresponding COL2A1 gene expression values for Figure 2 with cycle threshold (Ct) averages and GAPDH averages.

COL2A1 Gene Expression				
Sample	2^-ΔΔCt	std. dev.	Ct avg.	GAPDH avg.
(-) TNFα	1.00	0.11	19.21	23.37
(-)TNFα + PPS-MS (20μg/mL)	1.15	0.18	19.18	22.80
(+)TNFα	0.30	0.03	20.37	23.52
(+)TNFα + PPS-MS (2.5μg/mL)	0.22	0.02	21.19	23.08
(+)TNFα + PPS-MS (5μg/mL)	0.23	0.01	21.16	22.83
(+)TNFα + PPS-MS (10μg/mL)	0.26	N/A	20.38	22.59
(+)TNFα + PPS-MS (20μg/mL)	0.31	0.02	20.61	23.19

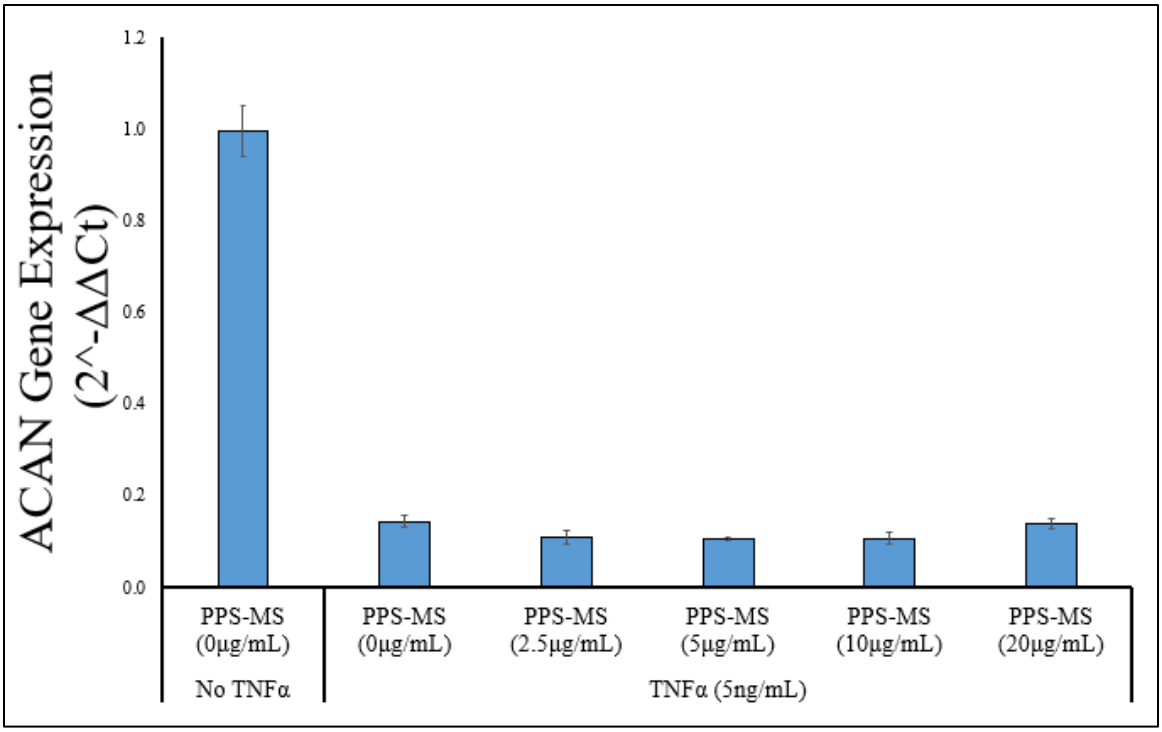

Figure 3: Graph shows ACAN gene expression for chondrocytes stimulated with TNFα normalized to GAPDH. n = 3 for most groups; n = 2 for TNFα (5ng/mL) + PPS-MS (2.5µg/mL); n = 2 for TNFα (5ng/mL) + PPS-MS (10µg/mL). All cells stimulated with TNFα were significantly different from control ($p < 0.001$). No significant differences were detected between TNFα stimulated cells treated with PPS-MS and non-treated cells. Bars represent mean and error bars represent standard deviation. One-way ANOVA with Holm-Sidak corrections were used to determine significance.

Table 2: Corresponding ACAN gene expression values for Figure 3 with cycle threshold (Ct) averages and GAPDH averages.

ACAN Gene Expression				
Sample	2^-ΔΔCt	std. dev.	Ct avg.	GAPDH avg.
(-) TNFα	1.00	0.06	22.37	23.37
(-) TNFα + PPS-MS (20μg/mL)	1.10	0.33	22.41	22.80
(+) TNFα	0.14	0.01	24.59	23.52
(+) TNFα + PPS-MS (2.5μg/mL)	0.11	0.01	25.38	23.08
(+) TNFα + PPS-MS (5μg/mL)	0.11	0.004	25.39	22.83
(+) TNFα + PPS-MS (10μg/mL)	0.11	0.01	25.02	22.59
(+) TNFα + PPS-MS (20μg/mL)	0.14	0.01	24.91	23.19

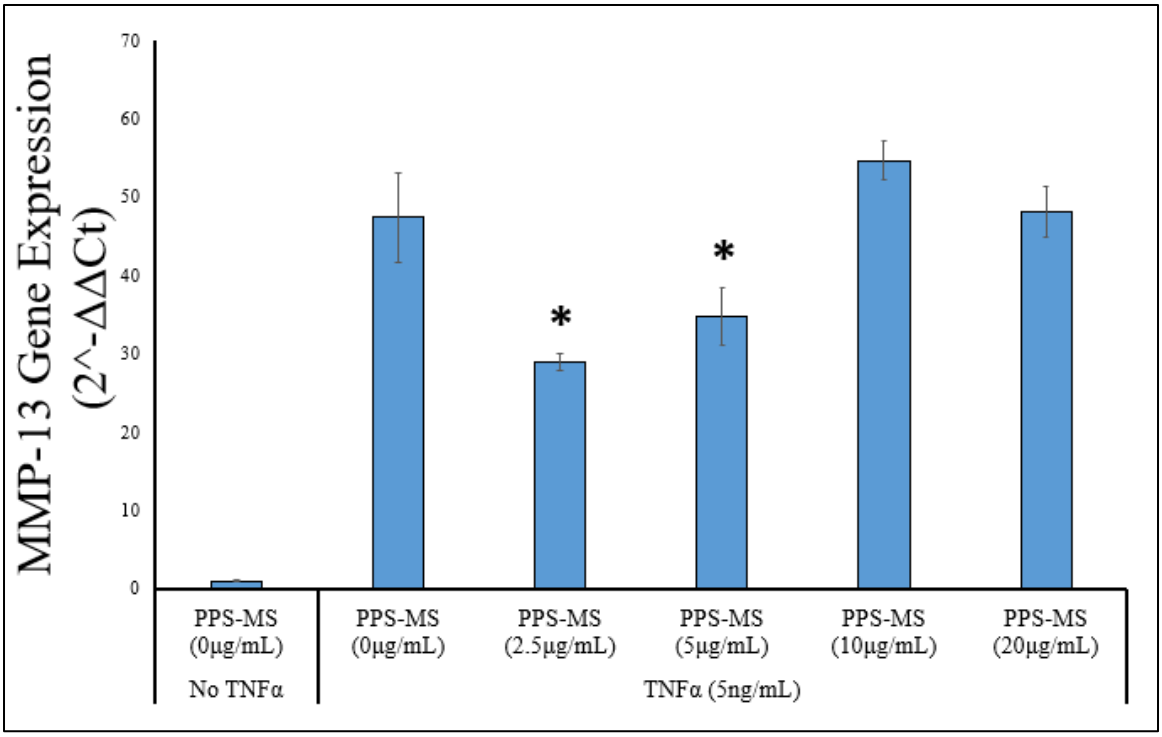

Figure 4: Graph shows MMP-13 gene expression for TNFα stimulated chondrocytes normalized to GAPDH. n = 3 for most groups; n = 2 for TNFα (5ng/mL) + PPS-MS (2.5µg/mL). All cells stimulated with TNFα were significantly different from control ($p < 0.001$). * indicates $p < 0.01$ compared to TNFα (5ng/mL) without PPS-MS. Bars represent mean and error bars represent standard deviation. One-way ANOVA with Holm-Sidak corrections were used to determine significance.

Table 3: Corresponding MMP-13 gene expression values for Figure 4 with cycle threshold (Ct) averages and GAPDH averages.

MMP-13 Gene Expression				
Sample	2^-ΔΔCt	std. dev.	Ct avg.	GAPDH avg.
(-) TNFα	1.00	0.14	31.71	23.37
(+) TNFα	47.40	5.74	25.58	23.80
(+) TNFα + PPS-MS (2.5μg/mL)	28.95	1.13	26.68	23.19
(+) TNFα + PPS-MS (5.0μg/mL)	34.78	3.61	26.39	22.83
(+) TNFα + PPS-MS (10μg/mL)	54.67	2.49	25.40	23.17
(+) TNFα + PPS-MS (20μg/mL)	48.14	3.18	25.85	23.10

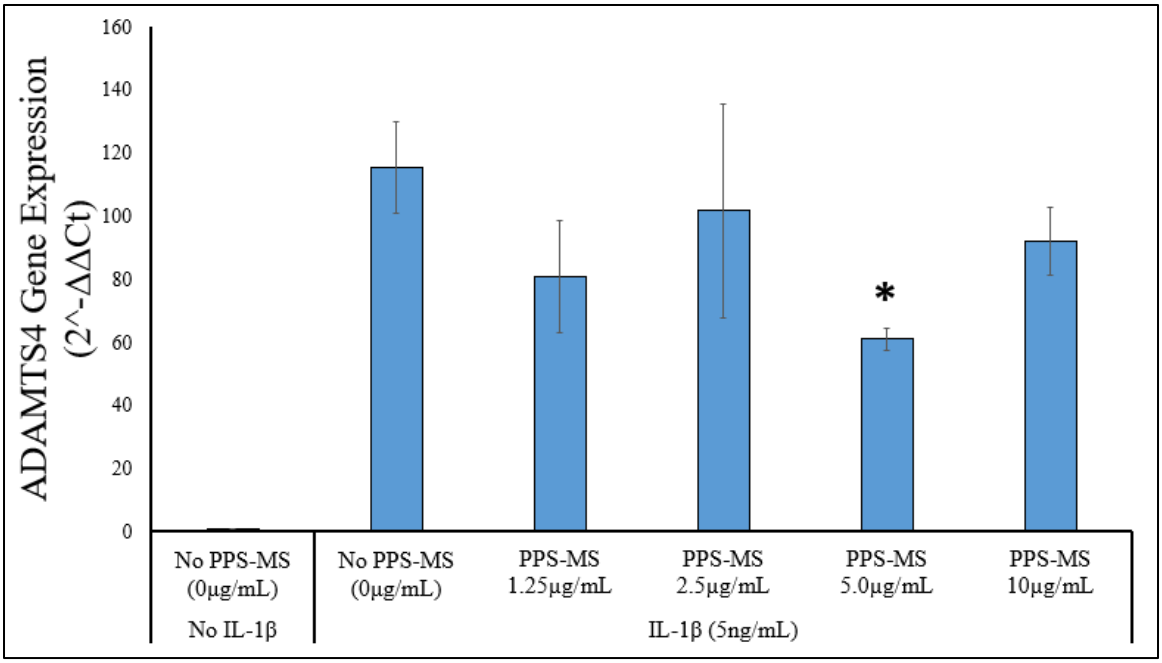

Figure 5: Graph shows ADAMTS4 gene expression for IL-1β stimulated chondrocytes normalized to GAPDH. n = 3 for all groups. All cells stimulated with IL-1β were significantly different from control ($p < 0.01$). * indicates $p<0.05$ compared to IL-1β (5ng/mL) stimulated cells without PPS-MS. Error bars show standard deviations. Bars represent mean and error bars represent standard deviation. One-way ANOVA with Holm-Sidak corrections were used to determine significance.

Table 4: Corresponding ADAMTS4 gene expression values for Figure 5 with cycle threshold (Ct) averages and GAPDH averages

ADAMTS4 Gene Expression				
Sample	2^-ΔΔCt	std. dev.	Ct avg.	GAPDH avg.
(-) IL-1β	1.00	0.08	32.70	21.64
(+) IL-1β	115.41	14.41	25.01	21.16
(+) IL-1β + PPS-MS (1.25μg/mL)	80.85	17.82	25.86	21.55
(+) IL-1β + PPS-MS (2.5μg/mL)	101.58	33.70	25.24	20.86
(+) IL-1β + PPS-MS (5μg/mL)	60.96	3.44	26.27	21.34
(+) IL-1β + PPS-MS (10μg/mL)	91.99	10.80	25.64	21.48

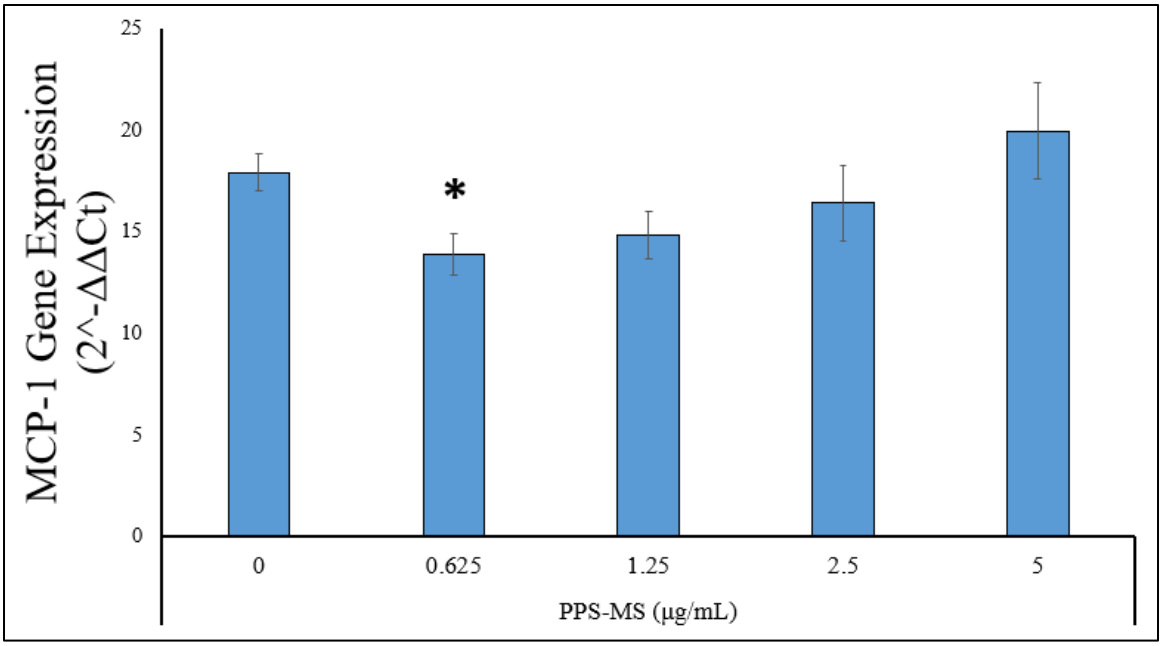

Figure 6: Graph shows MCP-1 gene expression for IL-1β stimulated chondrocytes normalized to GAPDH. n = 3 for all groups. All groups stimulated with 5ng/mL IL-1β. * indicates $p<0.08$ compared to no PPS-MS. Bars represent mean and error bars represent standard deviation. Unstimulated control not shown. One-way ANOVA with Holm-Sidak corrections were used to determine significance.

Table 5: Corresponding MCP-1 gene expression values for Figure 6 with cycle threshold (Ct) averages and GAPDH averages

MCP-1 Gene Expression				
Sample	2^-ΔΔCt	std. dev.	Ct avg.	GAPDH avg.
(-) IL-1β	1.40	1.42	26.10	22.84
(+) IL-1β	17.91	0.89	22.22	23.12
(+) IL-1β + PPS-MS (0.625μg/mL)	13.87	1.05	22.67	23.20
(+) IL-1β + PPS-MS (1.25μg/mL)	14.84	1.15	22.49	23.12
(+) IL-1β + PPS-MS (2.5μg/mL)	16.39	1.85	22.25	23.02
(+) IL-1β + PPS-MS (5.0μg/mL)	19.95	2.36	21.87	22.93

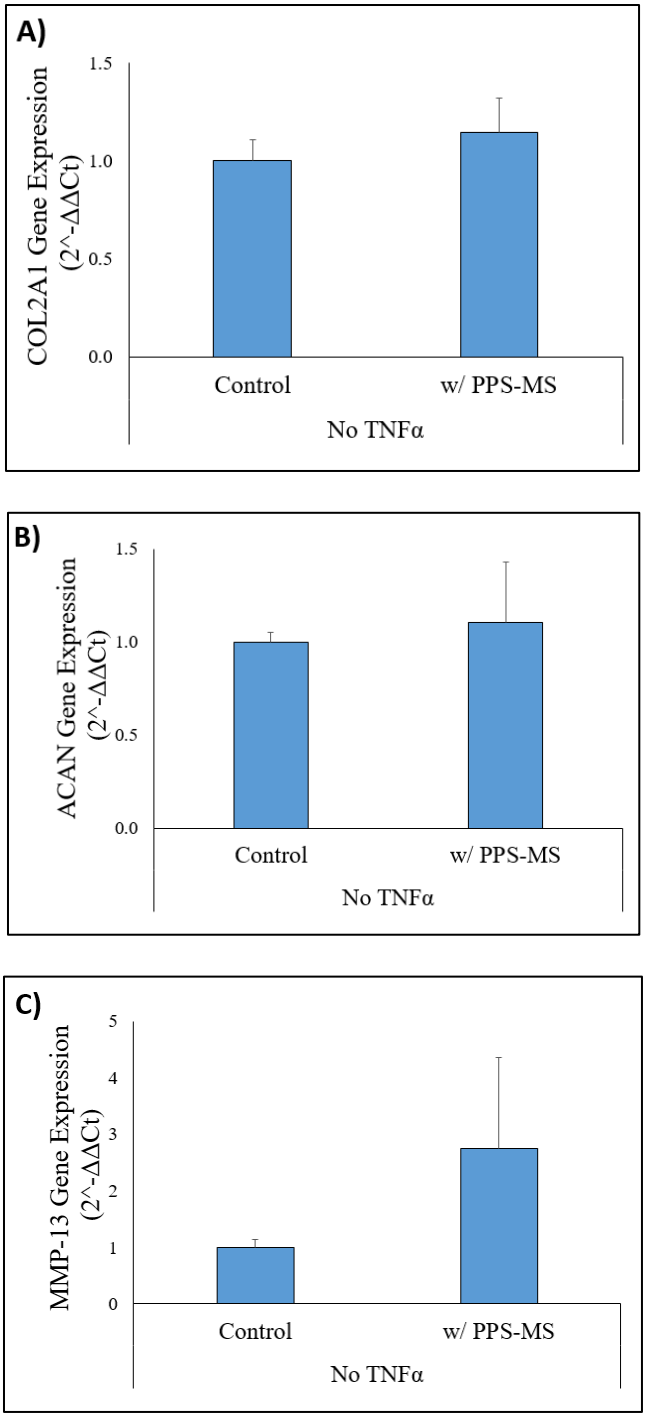

Figure 7: Graphs show gene expression data for unstimulated controls compared to cells treated with 20µg/mL of PPS-MS in the absence of TNFα for A) COL2A1, B) ACAN, and C) MMP-13. n = 3 for all groups with bars representing mean and error bars representing standard deviation. Student's t-test used to determine significance.

IL-1β Stimulated Chondrocytes Indirectly Co-Cultured with ADSCs

Gene expressions studied in this experiment were MMP-13, ACAN, and COL2A1. Following IL-1β stimulation, MMP-13 gene expression was increased nearly 8-fold, but co-culturing cytokine-stimulated cells with ADSCs did not significantly reduce expression (Figure 8). Due to the high variability in MMP-13 gene expression for unstimulated control, the 2^-ΔΔCt value is not equal to 1.00 (Table 6). Furthermore, anabolic expressions of ACAN and COL2A1 were found to decrease after cytokine stimulation. ADSCs were unsuccessful in recovering the loss of anabolic protein expressions (Figures 9 and 10) and show no detectable difference from cytokine-stimulated cells.

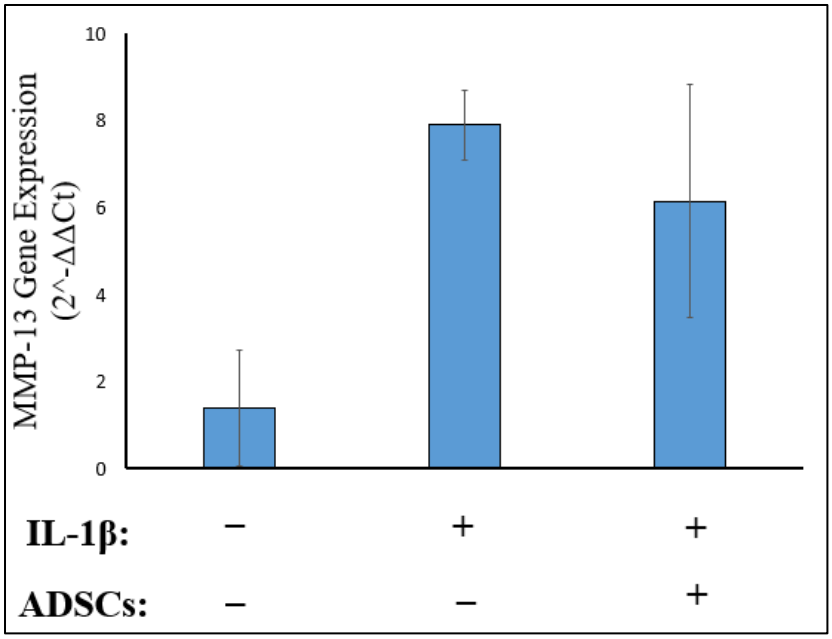

Figure 8: Graph shows MMP-13 gene expression, normalized to GAPDH, from chondrocytes stimulated with IL-1β (5ng/mL) then co-cultured indirectly with ADSCs for 24 hours. All cells stimulated with IL-1β were significantly different from control ($p < 0.05$), and there were no detected differences for the groups treated with ADSCs. Bars represent mean and error bars represent standard deviation with n = 3 samples per group. One-way ANOVA with Holm-Sidak corrections were used to determine significance.

Table 6: Corresponding MMP-13 gene expression values for Figure 8 with cycle threshold (Ct) averages and GAPDH averages.

MMP-13 Gene Expression				
Sample	2^-ΔΔCt	std. dev.	Ct avg.	GAPDH avg.
(-) IL-1β	1.39	1.34	29.20	21.76
(+) IL-1β	7.91	0.80	25.70	21.24
(+) IL-1β + ADSCs	6.15	2.69	26.24	21.32

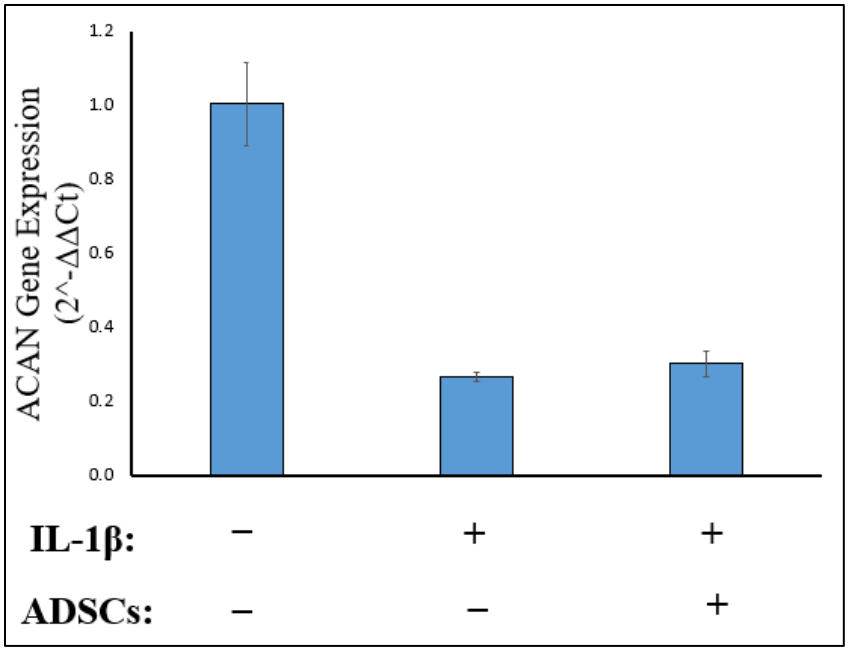

Figure 9: Graph shows ACAN gene expression, normalized to GAPDH, from chondrocytes stimulated with IL-1β (5ng/mL) then co-cultured indirectly with ADSCs for 24 hours. Bars represent mean and error bars represent standard deviation with n = 3 samples per group. All cells stimulated with IL-1β were significantly different from control ($p < 0.05$), and there were no detected differences for the groups treated with ADSCs. Kruskal-Wallis one-way ANOVA used to determine significance with Tukey post hoc test.

Table 7: Corresponding ACAN gene expression values for Figure 9 with cycle threshold (Ct) averages and GAPDH averages.

ACAN Gene Expression				
Sample	2^-ΔΔCt	std. dev.	Ct avg.	GAPDH avg.
(-) IL-1β	1.00	0.11	20.08	21.76
(+) IL-1β	0.27	0.01	21.47	21.24
(+) IL-1β + ADSCs	0.30	0.03	21.38	21.32

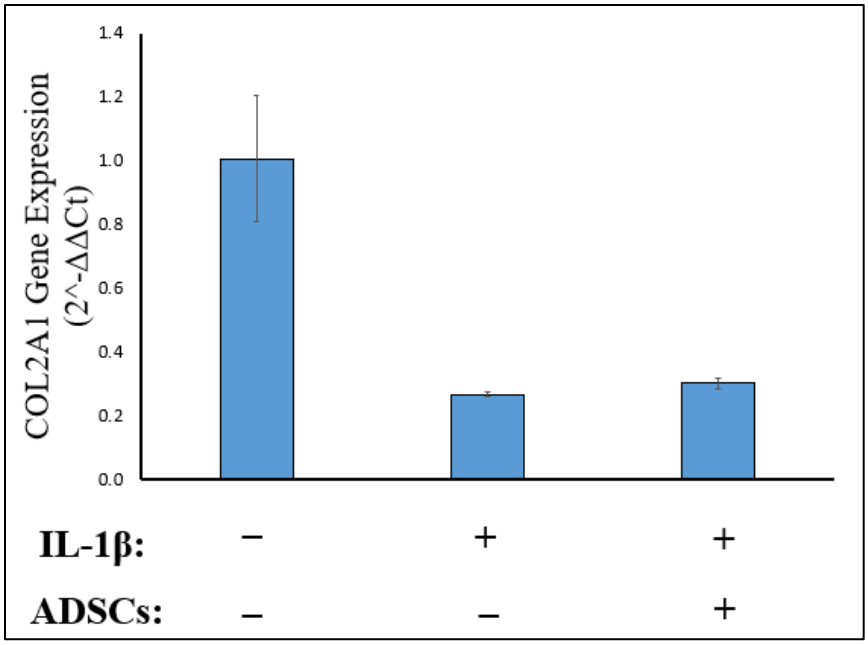

Figure 10: Graph shows COL2A1 gene expression, normalized to GAPDH, from chondrocytes stimulated with IL-1β (5ng/mL) then co-cultured indirectly with ADSCs for 24 hours. Bars represent mean and error bars represent standard deviation with n = 3 samples per group. All cells stimulated with IL-1β were significantly different from control ($p < 0.05$), and there were no detected differences for the groups treated with ADSCs. Kruskal-Wallis one-way ANOVA used to determine significance with Tukey post hoc test.

Table 8: Corresponding COL2A1 gene expression values for Figure 10 with cycle threshold (Ct) averages and GAPDH averages.

COL2A1 Gene Expression				
Sample	2^-ΔΔCt	std. dev.	Ct avg.	GAPDH avg.
(-) IL-1β	1.01	0.20	18.00	21.76
(+) IL-1β	0.14	0.01	20.33	21.24
(+) IL-1β + ADSCs	0.17	0.02	20.16	21.32

Oxidative Stress Impact on ADSCs with PPS-MS treatment

A preliminary experiment to determine the LD_{50} of ADSCs to hydrogen peroxide was performed and determined to be 500μM after 24 hours of culturing time (Figure 11). Using the established LD_{50} of hydrogen peroxide, a dose response to varying PPS-MS concentrations was performed. Comparing viability results against ADSCs cultured with hydrogen peroxide that did not receive PPS-MS treatment, statistically significant results were determined ($p<0.001$) for PPS-MS treated groups at concentrations of 1.0μg/mL, 2.1μg/mL, 4.2μg/mL, and 16.7μg/mL (Figure 12B). There was no significant change detected in viability for vehicle control of cells treated with PPS-MS but not cultured with hydrogen peroxide (Figure 12A). In examining the effect that cell number has on the LD_{50}, the data from figure 13 show that the addition of more cells results in an elevated LD_{50} for hydrogen peroxide. At 500μM H_2O_2, $5.0x10^3$ ADSCs had a viability of 66.1 ± 1.4% while the $1.0x10^4$ ADSCs had a viability of 78.4 ± 4.2%.

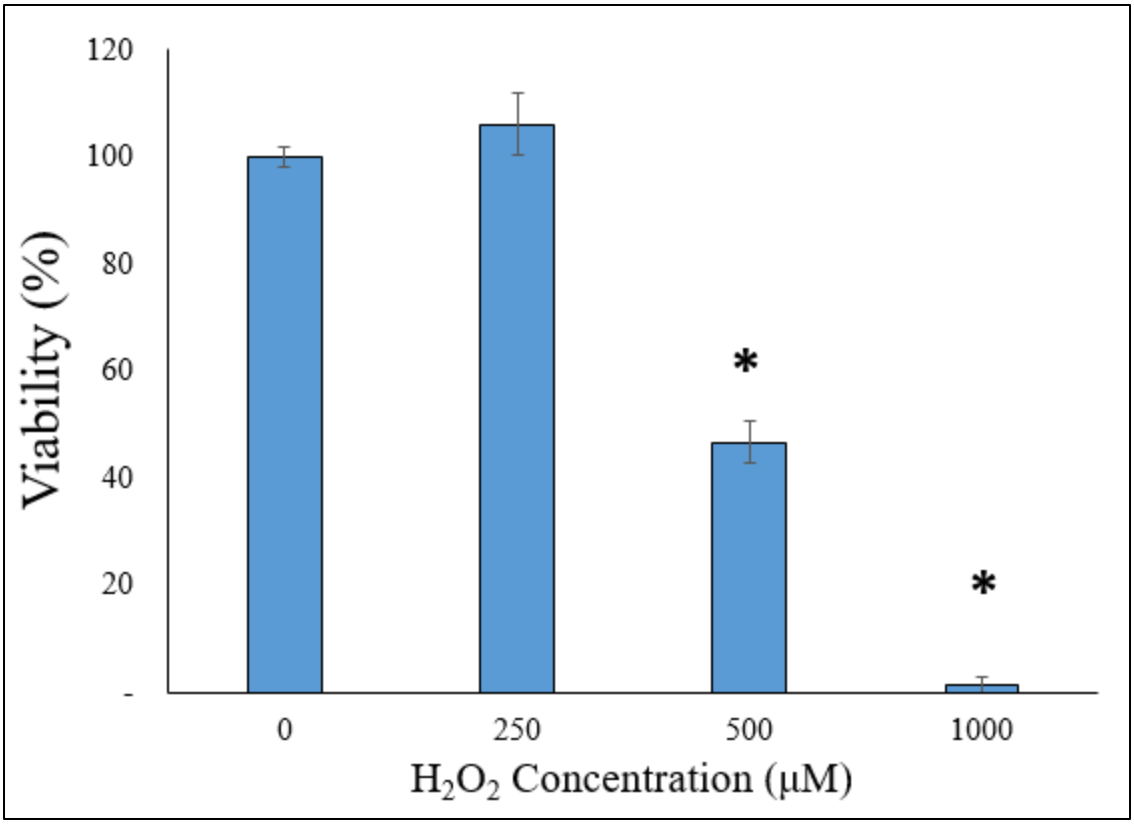

Figure 11: Graph shows the viability of ADSCs after 24 hours of hydrogen peroxide stimulation. Relative luminescence units, measuring ATP as an indicator of viability, were compared to 0µM H_2O_2 after treatment with increasing amounts of H_2O_2 to determine viability percentage. Bars represent mean and error bars represent standard deviation with n = 3 samples per group. Asterisk represents $p<0.001$ compared to 0µM H_2O_2. One-way ANOVA with Holm-Sidak corrections were used to determine significance.

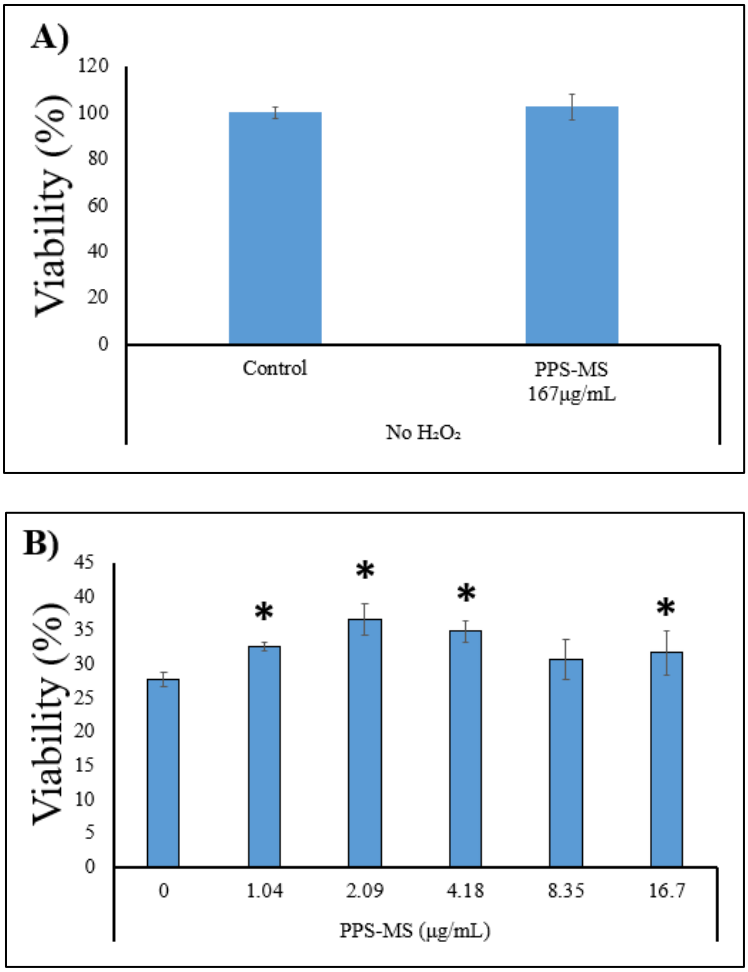

Figure 12: Graphs show viability assay of ADSCs with PPS-MS treatment in the presence of hydrogen peroxide. A) The graph shows the comparison of viability between control and vehicle in the absence of hydrogen peroxide. B) The graph shows viability of chondrocytes cultured in 500µM H_2O_2 with various concentrations of PPS-MS. Bars represent mean and error bars represent standard deviation with n = 4 samples per group. * represents $p < 0.001$ compared to 0µg PPS-MS /mL. One-way ANOVA with Holm-Sidak corrections were used to determine significance.

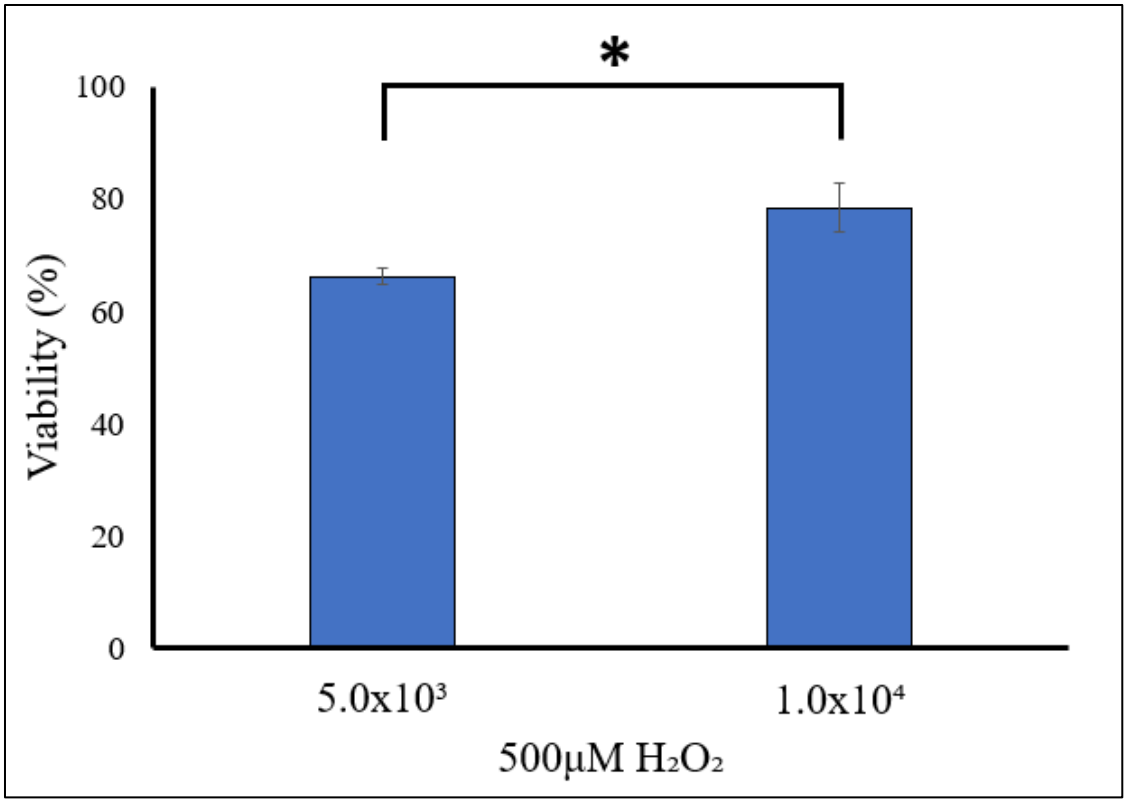

Figure 13: Graph shows cell viability based on cell number. Cell-Titer Glo viability assay at 500μM H_2O_2 comparing number of ADSCs ($5.0x10^3$ or $1.0x10^4$) after 24 hours of hydrogen peroxide stimulation. To determine viability percentage, relative luminescence units, measurements of ATP, were normalized to each group's control. Bars represent mean and error bars represent standard deviation with n = 3 samples per group. Asterisk represents $p<0.01$. Significance determined by Student's t-test.

Chondrocytes Pretreated with PPS-MS then co-cultured with ADSCs for 5 days

Three genes from chondrocytes were examined in this experiment: MMP-13, COL2A1, and Nox4 (NADPH oxidase 4). Two reference genes were also measured (GAPDH and β-actin, not shown). Because GAPDH was found to be more stable at day 0 and day 5, genes were normalized to this reference gene.

Analysis of MMP-13 shows a large increase (965-fold, data not shown) by the end of the stimulation period which drops considerably after removal of stimulus though the level remains relatively elevated at day 5 compared to controls (Figure 14A). Continued culture of the unstimulated controls over the course of 5 days shows significant 5-fold increase in MMP-13 gene expression. Stimulated chondrocytes that were co-cultured with ADSCs and treated with PPS-MS had significantly higher MMP-13 gene expression compared to monocultured stimulated chondrocytes treated with PPS-MS. Significance of the addition of PPS-MS during the stimulation period had no effect between stimulated groups. (Figure 15). There is a large variability in the stimulated chondrocytes in co-culture without PPS-MS and thus it has a p-value of 0.07 compared to stimulated chondrocytes in monoculture without PPS-MS.

As with MMP-13 gene expression, COL2A1 gene expression from unstimulated chondrocytes changes throughout the course of the study. COL2A1 decreased by 50% within 5 days (Figure 14B) with additional decreases to a value of 12% from the cytokine stimulation. ADSC co-culturing further reduced COL2A1 expression from stimulated chondrocytes (Figure 16). Gene expression for Day 0 stimulated chondrocytes was unable to be measured for COL2A1.

By day 5, Nox4 expression was elevated near 2-fold in stimulated chondrocytes (Figure 14C). By day 5 stimulated chondrocytes had higher Nox4 expressions than unstimulated chondrocytes ($p < 0.01$). The addition of ADSCs to stimulated chondrocytes prevented elevations in Nox4 gene expression due to stimulus and even further reduced expression beyond day 5 unstimulated controls (Figure 17). PPS-MS appeared to have no effect for any genes studied.

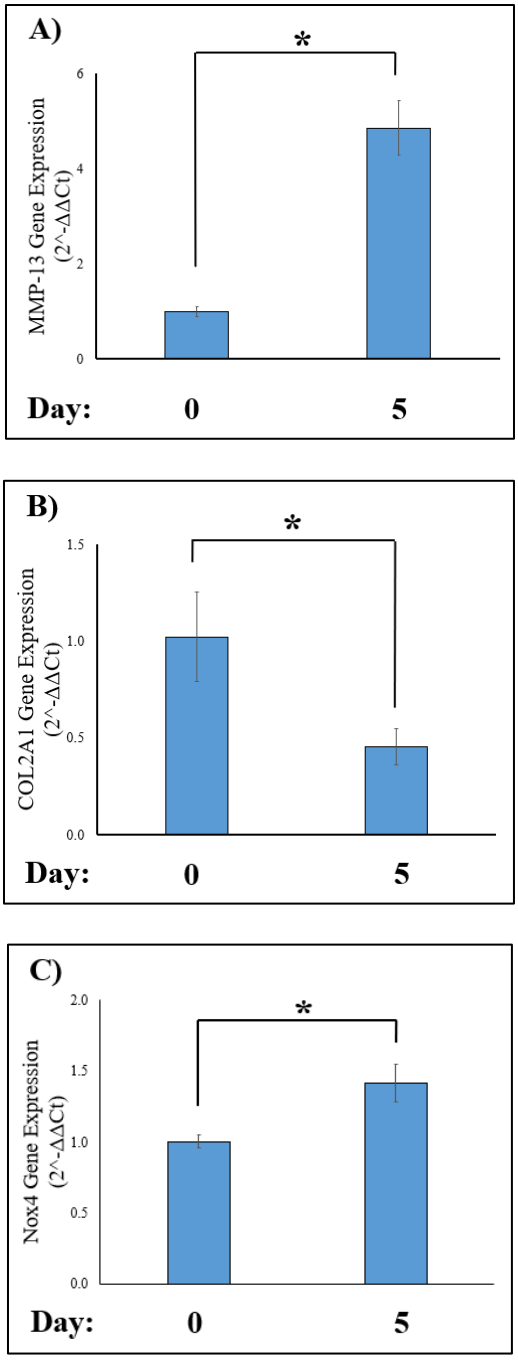

Figure 14: Graphs show gene expression data comparisons between day 0 (start of the stimulation period) and day 5 unstimulated and untreated controls. A) MMP-13. B) COL2A1. C) Nox4. Bars show mean and error bars are standard deviation with n = 4 samples ($p < 0.05$) Statistical analysis performed using non-parametric 2-tailed t-test for unequal variance (Welch's method).

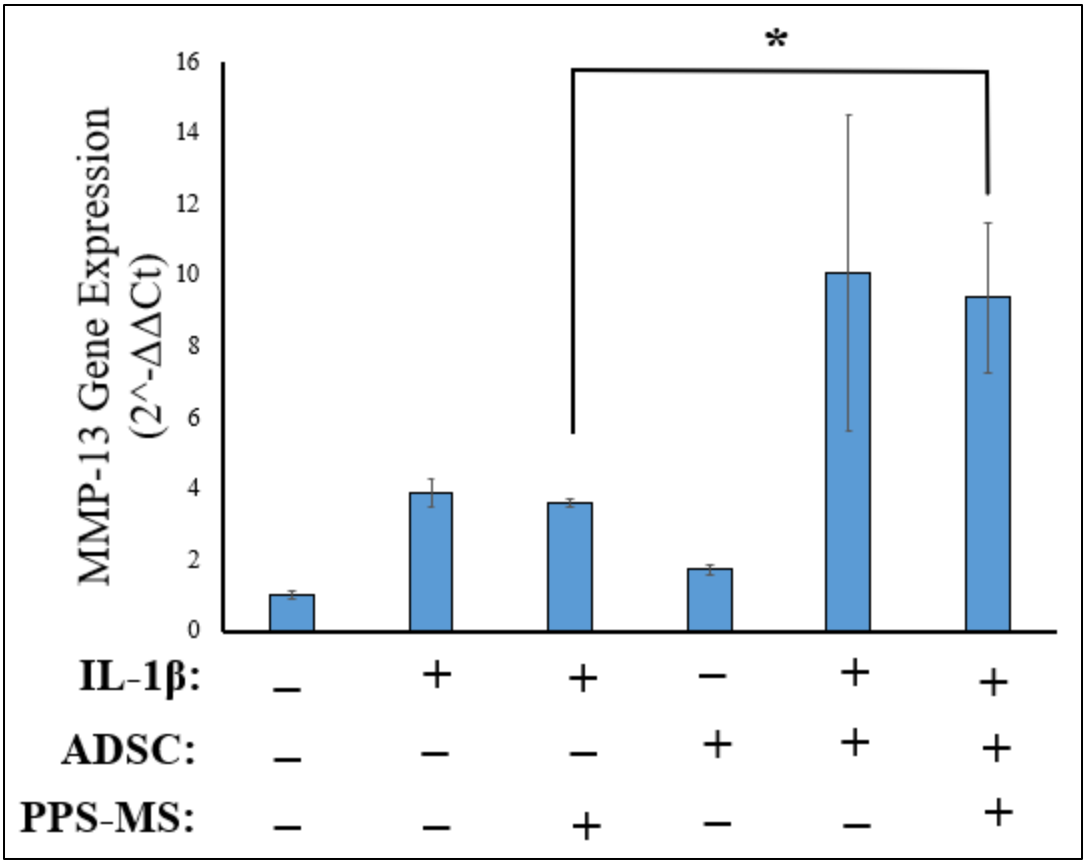

Figure 15: Graph shows MMP-13 gene expression from chondrocytes at day 5 normalized to GAPDH. All groups were significantly different from unstimulated and untreated control ($p < 0.05$). * indicates $p < 0.05$ compared to IL-1β stimulated chondrocytes + PPS-MS. Bars represent mean and error bars represent standard deviation with $n = 4$ samples per group. Gene expression is in reference to day 5 unstimulated. Statistical analysis performed using non-parametric 2-tailed t-test for unequal variance (Welch's method) with Bonferroni corrections.

Table 9: Corresponding MMP-13 gene expression values for Figure 15 with cycle threshold (Ct) averages and GAPDH averages

MMP-13 Gene Expression				
Sample	2^-ΔΔCt	std. dev.	Ct avg.	GAPDH avg.
Day 5: Unstimulated	1.01	0.12	27.70	21.88
Day 5: (+) IL-1β	3.88	0.41	25.63	21.76
Day 5: (+) IL-1β + PPS-MS	3.61	0.11	25.76	21.79
Day 5: Unstimulated + ADSCs	1.74	0.14	26.73	21.71
Day 5: (+) IL-1β + ADSCs	10.08	4.45	24.01	21.42
Day 5: (+) IL-1β + PPS-MS + ADSCs	9.39	2.10	24.14	21.53

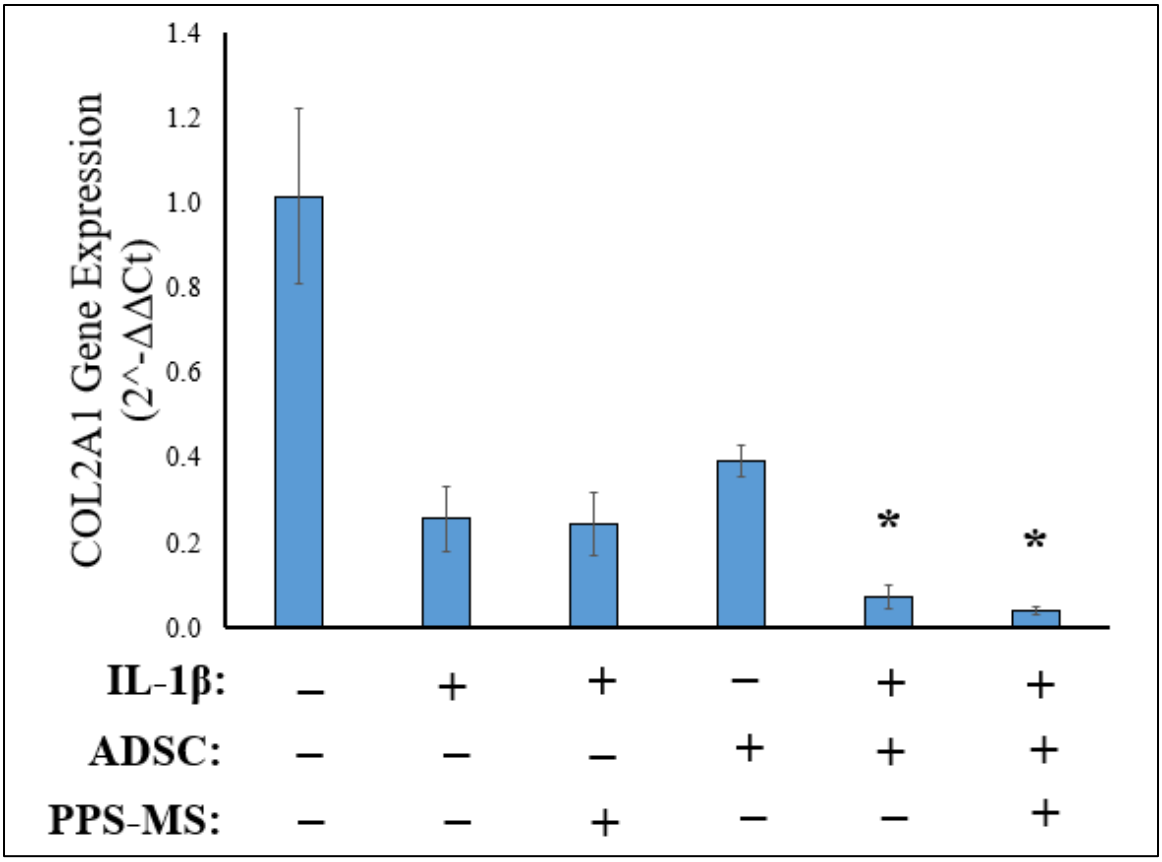

Figure 16: Graph shows COL2A1 gene expression from chondrocytes at day 5 normalized to GAPDH. All groups were significantly different from unstimulated and untreated control ($p < 0.01$). * indicates $p < 0.05$ compared to IL-1β stimulated chondrocytes. Unstimulated chondrocytes with ADSCs were not significantly different from stimulated chondrocytes. Bars represent mean and error bars represent standard deviation with n = 4 samples per group. Gene expression is in reference to day 5 unstimulated control. Statistical analysis performed using non-parametric 2-tailed t-test for unequal variance (Welch's method) with Bonferroni corrections.

Table 10: Corresponding COL2A1 gene expression values for Figure 16 with cycle threshold (Ct) averages and GAPDH averages

COL2A1 Gene Expression				
Sample	2^-ΔΔCt	std. dev.	Ct avg.	GAPDH avg.
Day 5: Unstimulated	1.01	0.21	22.79	21.88
Day 5: (+) IL-1β	0.26	0.08	24.69	21.76
Day 5: (+) IL-1β + PPS-MS	0.24	0.07	24.77	21.79
Day 5: Unstimulated + ADSCs	0.39	0.04	23.98	21.71
Day 5: (+) IL-1β + ADSCs	0.07	0.03	26.25	21.42
Day 5: (+) IL-1β + PPS-MS + ADSCs	0.04	0.01	27.09	21.53

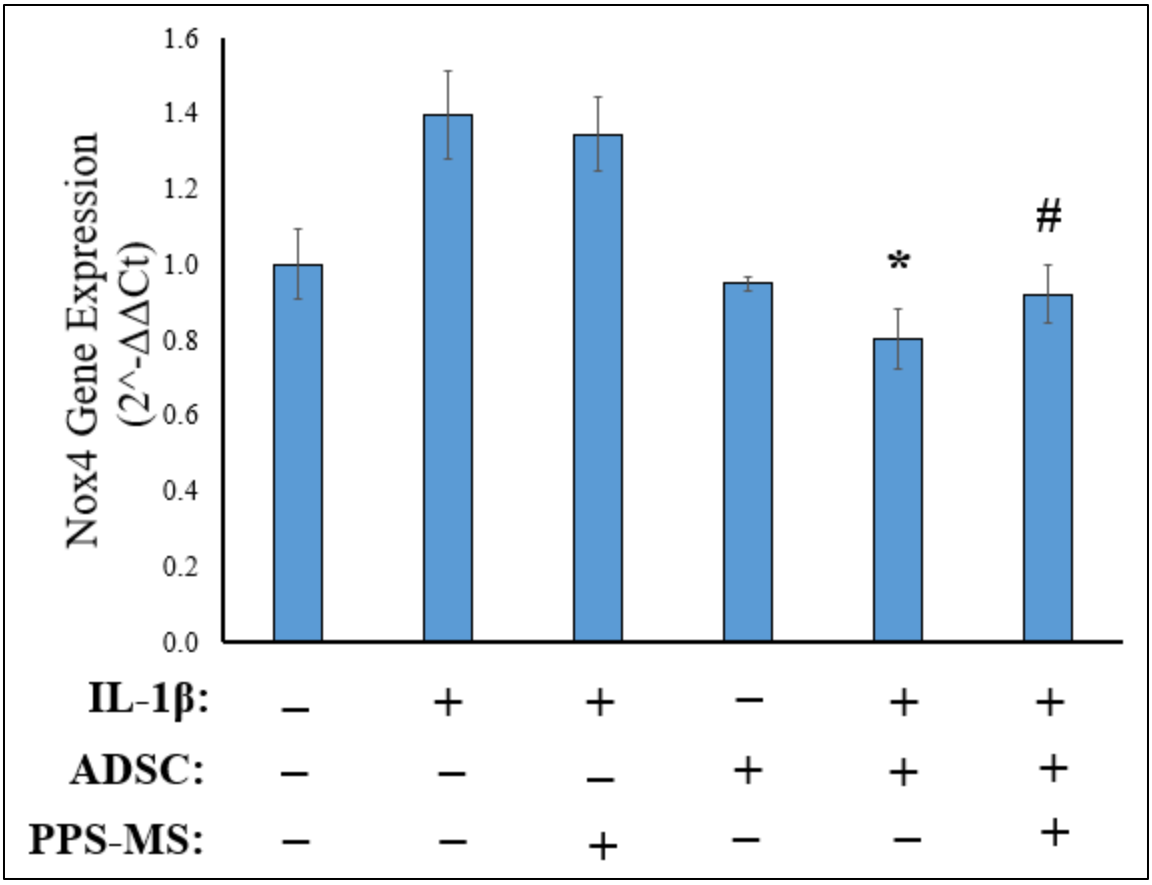

Figure 17: Graph shows Nox4 gene expression from chondrocytes at day 5 normalized to GAPDH. * indicates $p < 0.01$ compared to stimulated and untreated control. # indicates $p < 0.01$ compared to stimulated and PPS-MS treated control. Unstimulated groups are different from stimulated groups, but asterisk not shown above. Bars represent mean and error bars represent standard deviation with $n = 4$ samples per group. Gene expression is in reference to day 5 unstimulated control. Statistical analysis performed using non-parametric 2-tailed t-test for unequal variance (Welch's method) with Bonferroni corrections.

Table 11: Corresponding Nox4 gene expression values for Figure 17 with cycle threshold (Ct) averages and GAPDH averages

Nox4 Gene Expression				
Sample	2^-ΔΔCt	std. dev.	Ct avg.	GAPDH avg.
Day 5: Unstimulated	1.00	0.09	29.62	21.88
Day 5: (+) IL-1β	1.40	0.12	29.03	21.76
Day 5: (+) IL-1β + PPS-MS	1.35	0.10	29.10	21.79
Day 5: Unstimulated + ADSCs	0.95	0.02	29.53	21.71
Day 5: (+) IL-1β + ADSCs	0.80	0.08	29.48	21.42
Day 5: (+) IL-1β + PPS-MS + ADSCs	0.92	0.07	29.39	21.53

Discussion

Cytokine Stimulated Chondrocytes Treated with PPS-MS

Inflammatory conditions are mediated by the activation of transcription factors NF-kB to produce a variety of cytokines and chemokines, namely TNFα and IL-1β. These pro-inflammatory mediators act on the chondrocytes and surrounding cells to produce more inflammatory mediators and catabolic proteases through AP-1. The catabolic metalloproteinase MMP-13 is the most elevated MMP in OA and leads to degradation of type II collagen (COL2A1), the primary structural protein in articular cartilage [78]. Monocyte chemoattractant protein-1 also known as C-C chemokine lignad-2 (MCP-1 / CCL2) is a cytokine that leads to the attraction of monocytes into the joint synovium to become resident macrophages which will lead to further inflammation [79]. ACAN is a proteoglycan that is responsible for the water retention and shock

absorption properties of cartilage. A decrease in the synthesis of anabolic proteins is undesirable and contributes to progressive loss of cartilage as seen from OA patients.

To investigate the therapeutic benefit of PPS-MS, multiple experiments were conducted with cytokine stimulated chondrocytes treated with PPS-MS. Inflammatory cytokines increase MMP-13 gene expression, but the present data show that this response can be attenuated in the presence of PPS-MS. PPS-MS concentration at 2.5μg/mL resulted in decreased MMP-13 expressions; however, there were issues with reproducibility between experiments which may be due to inconsistencies in the PPS-MS concentration after reconstituting or in the number of cells plated. Although PPS-MS reduced catabolic expression of MMP-13, there was no recovery observed for the loss of anabolic expressions COL2A1 or ACAN, suggesting that decrease in expression of these genes is due to pathways that are not impacted by oxidative species scavenged by PPS-MS. Expression of other genes measured from IL-1β stimulated chondrocytes were MCP-1 and ADAMTS4. MCP-1 contributes to synovitis while ADAMTS4 is another metalloproteinase with a thrombospondin motif that cleaves the matrix proteoglycan aggrecan. Elevation of both ADAMTS4 and MCP-1 were also attenuated with antioxidant PPS-MS treatment. This would be beneficial in the joint for impeding cartilage degradation in osteoarthritis, as less proteoglycan would be cleaved which in turn would attract fewer inflammatory monocytes to the area.

IL-1β Stimulated Chondrocytes Indirectly Co-Cultured with ADSCs

From the collected data it appears that there was no impact in ADSC co-cultures in terms of recovering anabolic expression or attenuating catabolic expression from stimulated chondrocytes. It is likely that 24 hours of co-culture is not sufficient enough

time to elicit substantial responses. In addition, indirect co-cultures were compared to direct co-cultures of which no difference was observed between groups (data not shown).

Genes studied in this experiment were limited to MMP-13, COL2A1, and ACAN and thus may not reflect entirely on the chondrocyte-ADSC relationship. Furthermore, the presence and activity of secretory proteins such as IL-6, IL-1, TGFβ, and TSG-6 were not examined in the ADSC which likely are important in regulating chondrocyte phenotype. However, TGFβ is secreted in a latent form that has to be proteolytically activated which does not occur *in vitro*. Interestingly, ADSCs themselves did not show expression of MMP-13 (data not shown).

Oxidative Stress Impact on ADSCs with PPS-MS Treatment

Oxidative stress induces apoptosis (controlled cell death) by increasing the permeability of the mitochondrial membrane resulting in a loss of cytochrome c that activates executioner caspase-3 leading to apoptosis [80]. Injecting ADSCs into an inflamed knee joint which has elevated ROS levels could reduce the effectivity of ADSCs by inducing an apoptotic state. To overcome this undesirable interaction, PPS-MS was investigated for inhibition of hydrogen peroxide induced apoptosis.

The high concentration of hydrogen peroxide required to achieve an LD_{50} is physiologically impossible to generate [81] as cells typically produce local concentrations in the nanomolar range, the concentration was used in a follow-up experiment to determine if PPS-MS can protect from hydrogen peroxide induced cell death. At PPS-MS concentrations of 4.2μg/mL and below, the viability increased slightly but not enough to provide any superior protection from cell death. Because only cell viability was measured

and not caspase activation, it cannot be stated with certainty that apoptosis was the method for achieving cell death [82].

Additionally, the data from figure 13 show that the oxidative stress on cells is dependent on the cell number. This is intuitive as more stimulus should be required to elicit the same effect if more cells are plated. With twice as many ADSCs plated, the LD_{50} is required to be higher to achieve the same amount of cell death if there were fewer cells. Since cell number affects the oxidative environment, it could be a contributing factor to the variability observed for effective concentrations of PPS-MS treatments shown later on.

Chondrocytes Pretreated with PPS-MS then co-cultured with ADSCs for 5 days

Three genes from chondrocytes were examined in this experiment: catabolic protease MMP-13, anabolic matrix protein COL2A1, and ROS producer Nox4 (NADPH oxidase 4). Two reference genes, GAPDH and β-actin, were measured as well.

Regarding the use of PPS-MS, it does not appear that the concentration used had any effect for any gene expressions as Day 0 stimulated samples were no different from groups that received PPS-MS. It is likely that the narrow window of effective concentration was missed during the experiment. No conclusive claims can be made as to the effect of antioxidant pre-treatment on ADSC therapy.

During the stimulation period a large increase in MMP-13 was observed which subsided within 24 hours after removal of stimulus. The large increase in MMP-13 (965x) is likely due to the prolonged *in vitro* culture of the chondrocytes. As seen from unstimulated mono-layer cultures, baseline MMP-13 expression increases over time in culture indicating that older chondrocytes might be more susceptible to cytokine

stimulation causing overproduction of MMP-13. Increases in MMPs have been observed before *in vitro* [83] and with chondrocytes isolated from older donors [84]. In the present studies, samples from stimulated co-cultures treated with PPS-MS had significantly elevated MMP-13 expression compared to stimulated chondrocytes treated with PPS-MS in monoculture. Due to the large variation in the stimulated chondrocytes in co-culture without PPS-MS, they were not determined to be significantly different. However, From the evidence gathered it is apparent that ADSCs induce expression of MMP-13 from chondrocytes. MMP-13 was shown to induce osteogenesis from human MSCs which may accelerate bone regeneration after fracture [85]. The addition of ADSCs might result in a more fibrotic healing response from chondrocytes; however, because type I collagen expression was not measured from chondrocytes, no conclusions can be made regarding de-differentiation of chondrocytes or osteogenesis inducing conditions on ADSCs.

COL2A1 gene expression was greatly reduced with cytokine stimulation, but after cytokine removal, expression only recovered slightly by day 5. As the case with MMP-13, prolonged culture led to reduced chondrocyte expression of COL2A1 even with unstimulated groups. Comparisons of day 5 COL2A1 expression indicate that co-culturing unstimulated chondrocytes with ADSCs accelerates the loss of expression, which would not be beneficial for OA treatment. This reduced anabolic protein expression contradicts *in vivo* studies showing that ADSCs contribute to improved outcomes, indicating that COL2A1 expression may not be the best marker of chondrocyte health for this *in vitro* model or that the time response is not adequate [86, 87]. Alternatively, the loss of COL2A1 expression from chondrocytes may be caused by the

influence of anabolic factors produced by chondrocytes that act on ADSCs which reduce the levels of autocrine factors available for chondrocytes.

As demonstrated in experiments with COL2A1 and MMP-13, Nox4 expression in unstimulated controls changes over the 5-day culturing period. While correlation does not equal causation, it is interesting that the constitutively active producer of hydrogen peroxide increases expression as MMP-13 increases and COL2A1 decreases. However, the reduction in Nox4 expression from co-culture samples were not correlated with further reduction in MMP-13 or increases in COL2A1, but rather the opposite. As other investigators have reported, cytokine stimulation led to a reduction in Nox4 expression which was later elevated after removal of stimulus. In this experiment it was shown to remain elevated over non-stimulated controls up to five days after stimulus has been removed. Additionally, comparisons between day 5 samples of chondrocytes alone and co-cultures show that ADSC co-cultures prevent further elevation of Nox4 expression. This would be a beneficial action of ADSCs that prevent Nox4 expression from remaining chronically elevated. It is worthwhile to note that Nox4 expressions are extremely low, with cycle times (Ct) close to or exceeding 30.

Conclusion

Initial experiments solely involving PPS-MS and cytokine-stimulated chondrocytes show strong evidence for anti-inflammatory benefits from this antioxidant therapeutic. This is indicated by attenuation of catabolic proteases MMP-13 and ADAMTS4 along with the chemokine MCP-1. The most significant complication involving PPS-MS as a therapeutic is its very narrow range of effective concentration reflecting the negative and positive metabolic aspects of H_2O_2 in the cell. Because cells

are the producers of ROS, it is hypothesized that the effective concentration is more dependent on the ratio of cells to microspheres rather than the concentration of PPS-MS in the media. Given that there is likely a considerable amount of variability and a lack of precision or accuracy in cell plating, more or less cells could affect the effective PPS-MS concentration. Furthermore, it has been established that the LD_{50} of hydrogen peroxide is directly related to the cell number plated, and therefore, likely that PPS-MS will scavenge hydrogen peroxide produced by cells in a ratio appropriate to the number of cells in culture. This is also likely compounded by the narrow window of effective concentration that PPS-MS has; it is unknown if this narrow range is characteristic of PPS-MS or other antioxidant therapeutics as well.

The use of ADSCs as an anti-inflammatory were inconclusive. While MMP-13 was shown to consistently increase with co-culturing, expressions of chemokines and cytokines were not measured. Furthermore, the reduction in anabolic COL2A1 expression from chondrocytes may be due, in part, to an effect of growth factors secreted by chondrocytes. Although registering expression at high Ct values with PCR, the amount of constitutively active oxidant producer, Nox4, was significantly reduced at later time periods when co-cultured with ADSCs. This indicates a potentially beneficial response from ADSCs in reducing excessive ROS production by Nox4.

Due to the lack of change from PPS-MS treatment during the stimulation time, no conclusive evidence can be claimed regarding the state of antioxidant pretreatment for beneficial improvements in ADSC therapy. The genes examined through this research were selected due to their roles in cartilage damage and repair, but represent only a handful of the metabolome, and so should not be considered an exhaustive indicator for

OA pathogenesis. Lastly, ADSCs were only examined in regard to their impact on chondrocytes. Their use as an anti-inflammatory would suggest investigation into their interactions on immune cells such as macrophages. This reciprocal triangular response between chondrocytes, macrophages, and ADSCs which likely occurs *in vivo* could not be measured given the experimental set-up *in vitro*. Further investigations that should be considered are the interactions that macrophages have on chondrocytes and how ADSCs and/or PPS-MS would attenuate aggravation in this low-grade inflammatory model of OA.

References

1) Musumeci, G., Mobasheri, A., Trovato, F. M., Szychlinska, M. A., Imbesi, R., & Castrogiovanni, P. (2014). Post-operative rehabilitation and nutrition in osteoarthritis. *F1000Research*, *3*, 116. https://doi.org/10.12688/f1000research.4178.2

2) Wei, B., Du, X., Liu, J., Mao, F., Zhang, X., Liu, S., Xu, Y., Zang, F., & Wang, L. (2015). Associations between the properties of the cartilage matrix and findings from quantitative MRI in human osteoarthritic cartilage of the knee. *International journal of clinical and experimental pathology*, *8*(4), 3928–3936. .

3) Scanzello, C. R., & Goldring, S. R. (2012). The role of synovitis in osteoarthritis pathogenesis. *Bone*, *51*(2), 249–257. https://doi.org/10.1016/j.bone.2012.02.012

4) Riegger, J., & Brenner, R. E. (2020). Pathomechanisms of Posttraumatic Osteoarthritis: Chondrocyte Behavior and Fate in a Precarious Environment. *International journal of molecular sciences*, *21*(5), 1560. https://doi.org/10.3390/ijms21051560

5) Pereira, D., Ramos, E., & Branco, J. (2015). Osteoarthritis. *Acta medica portuguesa*, *28*(1), 99–106. https://doi.org/10.20344/amp.5477

6) Weber, M., Renkawitz, T., Voellner, F., Craiovan, B., Greimel, F., Worlicek, M., Grifka, J., & Benditz, A. (2018). Revision Surgery in Total Joint Replacement Is Cost-Intensive. *BioMed research international*, *2018*, 8987104. https://doi.org/10.1155/2018/8987104

7) Barrack, R. L., Hoffman, G. J., Tejeiro, W. V., & Carpenter, L. J., Jr (1995). Surgeon work input and risk in primary versus revision total joint arthroplasty. *The Journal of arthroplasty*, *10*(3), 281–286. https://doi.org/10.1016/s0883-5403(05)80175-5

8) Ghouri, A., & Conaghan, P. G. (2019). Update on novel pharmacological therapies for osteoarthritis. *Therapeutic advances in musculoskeletal disease*, *11*, 1759720X19864492. https://doi.org/10.1177/1759720X19864492

9) O'Grady, K. P., Kavanaugh, T. E., Cho, H., Ye, H., Gupta, M. K., Madonna, M. C., Lee, J., O'Brien, C. M., Skala, M. C., Hasty, K. A., & Duvall, C. L. (2018). Drug-Free ROS Sponge Polymeric Microspheres Reduce Tissue Damage from Ischemic and Mechanical Injury. *ACS biomaterials science & engineering*, *4*(4), 1251–1264. https://doi.org/10.1021/acsbiomaterials.6b00804

10) Bahrampour Juybari, K., Kamarul, T., Najafi, M., Jafari, D., & Sharifi, A. M. (2018). Restoring the IL-1β/NF-κB-induced impaired chondrogenesis by diallyl disulfide in human adipose-derived mesenchymal stem cells via attenuation of reactive oxygen species and elevation of antioxidant enzymes. *Cell and tissue research*, *373*(2), 407–419. https://doi.org/10.1007/s00441-018-2825-y

11) Poole, K. M., Nelson, C. E., Joshi, R. V., Martin, J. R., Gupta, M. K., Haws, S. C., Kavanaugh, T. E., Skala, M. C., & Duvall, C. L. (2015). ROS-responsive microspheres for on demand antioxidant therapy in a model of diabetic peripheral arterial disease. *Biomaterials*, *41*, 166–175. https://doi.org/10.1016/j.biomaterials.2014.11.016

12) Kaul, N., & Forman, H. J. (1996). Activation of NF kappa B by the respiratory burst of macrophages. *Free radical biology & medicine*, *21*(3), 401–405. https://doi.org/10.1016/0891-5849(96)00178-5
13) Pittenger, M. F., Discher, D. E., Péault, B. M., Phinney, D. G., Hare, J. M., & Caplan, A. I. (2019). Mesenchymal stem cell perspective: cell biology to clinical progress. *NPJ Regenerative medicine*, *4*, 22. https://doi.org/10.1038/s41536-019-0083-6
14) Abdelmawgoud, H., & Saleh, A. (2018). Anti-inflammatory and antioxidant effects of mesenchymal and hematopoietic stem cells in a rheumatoid arthritis rat model. *Advances in clinical and experimental medicine : official organ Wroclaw Medical University*, *27*(7), 873–880. https://doi.org/10.17219/acem/73720
15) Carballo, C. B., Nakagawa, Y., Sekiya, I., & Rodeo, S. A. (2017). Basic Science of Articular Cartilage. *Clinics in sports medicine*, *36*(3), 413–425. https://doi.org/10.1016/j.csm.2017.02.001
16) Bhosale, A. M., & Richardson, J. B. (2008). Articular cartilage: structure, injuries and review of management. *British medical bulletin*, *87*, 77–95. https://doi.org/10.1093/bmb/ldn025
17) Maroudas A. I. (1976). Balance between swelling pressure and collagen tension in normal and degenerate cartilage. *Nature*, *260*(5554), 808–809. https://doi.org/10.1038/260808a0
18) *JOSE, P., & HMMANSOU, R. (2003). Biomechanics of Cartilage.*
19) Adams, M. E., & Brandt, K. D. (1991). Hypertrophic repair of canine articular cartilage in osteoarthritis after anterior cruciate ligament transection. *The Journal of rheumatology*, *18*(3), 428–435.
20) van der Kraan, P. M., & van den Berg, W. B. (2012). Chondrocyte hypertrophy and osteoarthritis: role in initiation and progression of cartilage degeneration?. *Osteoarthritis and cartilage*, *20*(3), 223–232. https://doi.org/10.1016/j.joca.2011.12.003
https://doi.org/10.1016/j.joca.2011.12.003
21) Madry, H., Luyten, F. P., & Facchini, A. (2012). Biological aspects of early osteoarthritis. *Knee surgery, sports traumatology, arthroscopy : official journal of the ESSKA*, *20*(3), 407–422. https://doi.org/10.1007/s00167-011-1705-8
22) Mackie, E. J., Ahmed, Y. A., Tatarczuch, L., Chen, K. S., & Mirams, M. (2008). Endochondral ossification: how cartilage is converted into bone in the developing skeleton. *The international journal of biochemistry & cell biology*, *40*(1), 46–62. https://doi.org/10.1016/j.biocel.2007.06.009
23) Kohn, M. D., Sassoon, A. A., & Fernando, N. D. (2016). Classifications in Brief: Kellgren-Lawrence Classification of Osteoarthritis. *Clinical orthopaedics and related research*, *474*(8), 1886–1893. https://doi.org/10.1007/s11999-016-4732-4
24) Hügle, T., & Geurts, J. (2017). What drives osteoarthritis?-synovial versus subchondral bone pathology. *Rheumatology (Oxford, England)*, *56*(9), 1461–1471. https://doi.org/10.1093/rheumatology/kew389
25) Zhang, H., Cai, D., & Bai, X. (2020). Macrophages regulate the progression of osteoarthritis. *Osteoarthritis and cartilage*, *28*(5), 555–561. https://doi.org/10.1016/j.joca.2020.01.007

26) Pessler, F., Dai, L., Diaz-Torne, C., Gomez-Vaquero, C., Paessler, M. E., Zheng, D. H., Einhorn, E., Range, U., Scanzello, C., & Schumacher, H. R. (2008). The synovitis of "non-inflammatory" orthopaedic arthropathies: a quantitative histological and immunohistochemical analysis. *Annals of the rheumatic diseases*, *67*(8), 1184–1187. https://doi.org/10.1136/ard.2008.087775
27) Scanzello, C. R., Plaas, A., & Crow, M. K. (2008). Innate immune system activation in osteoarthritis: is osteoarthritis a chronic wound?. *Current opinion in rheumatology*, *20*(5), 565–572. https://doi.org/10.1097/BOR.0b013e32830aba34
28) Bondeson, J., Wainwright, S. D., Lauder, S., Amos, N., & Hughes, C. E. (2006). The role of synovial macrophages and macrophage-produced cytokines in driving aggrecanases, matrix metalloproteinases, and other destructive and inflammatory responses in osteoarthritis. *Arthritis research & therapy*, *8*(6), R187. https://doi.org/10.1186/ar2099
29) Kurz, B., Lemke, A. K., Fay, J., Pufe, T., Grodzinsky, A. J., & Schünke, M. (2005). Pathomechanisms of cartilage destruction by mechanical injury. *Annals of anatomy = Anatomischer Anzeiger : official organ of the Anatomische Gesellschaft*, *187*(5-6), 473–485. https://doi.org/10.1016/j.aanat.2005.07.003
30) Charlier, E., Relic, B., Deroyer, C., Malaise, O., Neuville, S., Collée, J., Malaise, M. G., & De Seny, D. (2016). Insights on Molecular Mechanisms of Chondrocytes Death in Osteoarthritis. *International journal of molecular sciences*, *17*(12), 2146. https://doi.org/10.3390/ijms17122146
31) Riegger, J., Joos, H., Palm, H. G., Friemert, B., Reichel, H., Ignatius, A., & Brenner, R. E. (2016). Antioxidative therapy in an ex vivo human cartilage trauma-model: attenuation of trauma-induced cell loss and ECM-destructive enzymes by N-acetyl cysteine. *Osteoarthritis and cartilage*, *24*(12), 2171–2180. https://doi.org/10.1016/j.joca.2016.07.019
32) Goodwin, W., McCabe, D., Sauter, E., Reese, E., Walter, M., Buckwalter, J. A., & Martin, J. A. (2010). Rotenone prevents impact-induced chondrocyte death. *Journal of orthopaedic research : official publication of the Orthopaedic Research Society*, *28*(8), 1057–1063. https://doi.org/10.1002/jor.21091
33) Jeffrey, J. E., Gregory, D. W., & Aspden, R. M. (1995). Matrix damage and chondrocyte viability following a single impact load on articular cartilage. *Archives of biochemistry and biophysics*, *322*(1), 87–96. https://doi.org/10.1006/abbi.1995.1439
34) Wolf, M., Lossdörfer, S., Craveiro, R., Götz, W., & Jäger, A. (2013). Regulation of macrophage migration and activity by high-mobility group box 1 protein released from periodontal ligament cells during orthodontically induced periodontal repair: an in vitro and in vivo experimental study. *Journal of orofacial orthopedics = Fortschritte der Kieferorthopadie : Organ/official journal Deutsche Gesellschaft fur Kieferorthopadie*, *74*(5), 420–434. https://doi.org/10.1007/s00056-013-0167-7
35) Barreto, G., Manninen, M., & K Eklund, K. (2020). Osteoarthritis and Toll-Like Receptors: When Innate Immunity Meets Chondrocyte Apoptosis. *Biology*, *9*(4), 65. https://doi.org/10.3390/biology9040065
36) Lambert, C., Borderie, D., Dubuc, J. E., Rannou, F., & Henrotin, Y. (2019). Type II collagen peptide Coll2-1 is an actor of synovitis. *Osteoarthritis and cartilage*, *27*(11), 1680–1691. https://doi.org/10.1016/j.joca.2019.07.009

37) Ma, P., Yue, L., Yang, H., Fan, Y., Bai, J., Li, S., Yuan, J., Zhang, Z., Yao, C., Lin, M., & Hou, Q. (2020). Chondroprotective and anti-inflammatory effects of amurensin H by regulating TLR4/Syk/NF-κB signals. *Journal of cellular and molecular medicine*, *24*(2), 1958–1968. https://doi.org/10.1111/jcmm.14893
38) Bianchi M. E. (2007). DAMPs, PAMPs and alarmins: all we need to know about danger. *Journal of leukocyte biology*, *81*(1), 1–5. https://doi.org/10.1189/jlb.0306164
39) Karin, M., & Delhase, M. (1998). JNK or IKK, AP-1 or NF-kappaB, which are the targets for MEK kinase 1 action?. *Proceedings of the National Academy of Sciences of the United States of America*, *95*(16), 9067–9069. https://doi.org/10.1073/pnas.95.16.9067
40) Blackwell, T. S., & Christman, J. W. (1997). The role of nuclear factor-kappa B in cytokine gene regulation. *American journal of respiratory cell and molecular biology*, *17*(1), 3–9. https://doi.org/10.1165/ajrcmb.17.1.f132
41) Oeckinghaus, A., & Ghosh, S. (2009). The NF-kappaB family of transcription factors and its regulation. *Cold Spring Harbor perspectives in biology*, *1*(4), a000034. https://doi.org/10.1101/cshperspect.a000034
42) Jenei-Lanzl, Z., Meurer, A., & Zaucke, F. (2019). Interleukin-1β signaling in osteoarthritis - chondrocytes in focus. *Cellular signalling*, *53*, 212–223. https://doi.org/10.1016/j.cellsig.2018.10.005
43) Hui, A., Min, W. X., Tang, J., & Cruz, T. F. (1998). Inhibition of activator protein 1 activity by paclitaxel suppresses interleukin-1-induced collagenase and stromelysin expression by bovine chondrocytes. *Arthritis and rheumatism*, *41*(5), 869–876. https://doi.org/10.1002
44) Nishina, H., Wada, T., & Katada, T. (2004). Physiological roles of SAPK/JNK signaling pathway. *Journal of biochemistry*, *136*(2), 123–126. https://doi.org/10.1093/jb/mvh117
45) Lepetsos, P., & Papavassiliou, A. G. (2016). ROS/oxidative stress signaling in osteoarthritis. *Biochimica et biophysica acta*, *1862*(4), 576–591. https://doi.org/10.1016/j.bbadis.2016.01.003
46) Lo, Y. Y., Wong, J. M., & Cruz, T. F. (1996). Reactive oxygen species mediate cytokine activation of c-Jun NH2-terminal kinases. *The Journal of biological chemistry*, *271*(26), 15703–15707. https://doi.org/10.1074/jbc.271.26.15703
47) Roberts, M. L., & Cowsert, L. M. (1998). Interleukin-1 beta and reactive oxygen species mediate activation of c-Jun NH2-terminal kinases, in human epithelial cells, by two independent pathways. *Biochemical and biophysical research communications*, *251*(1), 166–172. https://doi.org/10.1006/bbrc.1998.9434
48) Ursini, F., Maiorino, M., & Forman, H. J. (2016). Redox homeostasis: The Golden Mean of healthy living. *Redox biology*, *8*, 205–215. https://doi.org/10.1016/j.redox.2016.01.010
49) Berridge, M.J. (2014) Cell Signalling Biology; doi:10.1042/csb0001002
50) Imbert, V., Rupec, R. A., Livolsi, A., Pahl, H. L., Traenckner, E. B., Mueller-Dieckmann, C., Farahifar, D., Rossi, B., Auberger, P., Baeuerle, P. A., & Peyron, J. F. (1996). Tyrosine phosphorylation of I kappa B-alpha activates NF-kappa B without proteolytic degradation of I kappa B-alpha. *Cell*, *86*(5), 787–798. https://doi.org/10.1016/s0092-8674(00)80153-1

51) Davalli, P., Mitic, T., Caporali, A., Lauriola, A., & D'Arca, D. (2016). ROS, Cell Senescence, and Novel Molecular Mechanisms in Aging and Age-Related Diseases. *Oxidative medicine and cellular longevity*, *2016*, 3565127. https://doi.org/10.1155/2016/3565127
52) Brieger, K., Schiavone, S., Miller, F. J., Jr, & Krause, K. H. (2012). Reactive oxygen species: from health to disease. *Swiss medical weekly*, *142*, w13659. https://doi.org/10.4414/smw.2012.13659
53) Sies, H., & Jones, D. P. (2020). Reactive oxygen species (ROS) as pleiotropic physiological signalling agents. *Nature reviews. Molecular cell biology*, *21*(7), 363–383. https://doi.org/10.1038/s41580-020-0230-3
54) Eo, S. H., Cho, H., & Kim, S. J. (2013). Resveratrol Inhibits Nitric Oxide-Induced Apoptosis via the NF-Kappa B Pathway in Rabbit Articular Chondrocytes. *Biomolecules & therapeutics*, *21*(5), 364–370. https://doi.org/10.4062/biomolther.2013.029
55) Bentz, M., Zaouter, C., Shi, Q., Fahmi, H., Moldovan, F., Fernandes, J. C., & Benderdour, M. (2012). Inhibition of inducible nitric oxide synthase prevents lipid peroxidation in osteoarthritic chondrocytes. *Journal of cellular biochemistry*, *113*(7), 2256–2267. https://doi.org/10.1002/jcb.24096
56) Elbim, C., Bailly, S., Chollet-Martin, S., Hakim, J., & Gougerot-Pocidalo, M. A. (1994). Differential priming effects of proinflammatory cytokines on human neutrophil oxidative burst in response to bacterial N-formyl peptides. *Infection and immunity*, *62*(6), 2195–2201. https://doi.org/10.1128/IAI.62.6.2195-2201.1994
57) Bassal, S., Liu, Y. S., Thomas, R. J., & Phillips, W. A. (1997). Phosphotyrosine phosphatase activity in the macrophage is enhanced by lipopolysaccharide, tumor necrosis factor alpha, and granulocyte/macrophage-colony stimulating factor: correlation with priming of the respiratory burst. *Biochimica et biophysica acta*, *1355*(3), 343–352. https://doi.org/10.1016/s0167-4889(96)00149-8
58) Drapier, J. C., & Hibbs, J. B., Jr (1986). Murine cytotoxic activated macrophages inhibit aconitase in tumor cells. Inhibition involves the iron-sulfur prosthetic group and is reversible. *The Journal of clinical investigation*, *78*(3), 790–797. https://doi.org/10.1172/JCI112642
59) Cao, Y., Zhang, X., Shang, W., Xu, J., Wang, X., Hu, X., Ao, Y., & Cheng, H. (2013). Proinflammatory Cytokines Stimulate Mitochondrial Superoxide Flashes in Articular Chondrocytes In Vitro and In Situ. *PloS one*, *8*(6), e66444. https://doi.org/10.1371/journal.pone.0066444
60) Drevet, S., Gavazzi, G., Grange, L., Dupuy, C., & Lardy, B. (2018). Reactive oxygen species and NADPH oxidase 4 involvement in osteoarthritis. *Experimental gerontology*, *111*, 107–117. https://doi.org/10.1016/j.exger.2018.07.007
61) Rousset, F., Hazane-Puch, F., Pinosa, C., Nguyen, M. V., Grange, L., Soldini, A., Rubens-Duval, B., Dupuy, C., Morel, F., & Lardy, B. (2015). IL-1beta mediates MMP secretion and IL-1beta neosynthesis via upregulation of p22(phox) and NOX4 activity in human articular chondrocytes. *Osteoarthritis and cartilage*, *23*(11), 1972–1980. https://doi.org/10.1016/j.joca.2015.02.167

62) Wegner, A. M., Campos, N. R., Robbins, M. A., Haddad, A. F., Cunningham, H. C., Yik, J., Christiansen, B. A., & Haudenschild, D. R. (2019). Acute Changes in NADPH Oxidase 4 in Early Post-Traumatic Osteoarthritis. *Journal of orthopaedic research : official publication of the Orthopaedic Research Society*, *37*(11), 2429–2436. https://doi.org/10.1002/jor.24417
63) DeJulius, C. R., Bernardo-Colón, A., Naguib, S., Backstrom, J. R., Kavanaugh, T., Gupta, M. K., Duvall, C. L., & Rex, T. S. (2021). Microsphere antioxidant and sustained erythropoietin-R76E release functions cooperate to reduce traumatic optic neuropathy. *Journal of controlled release : official journal of the Controlled Release Society*, *329*, 762–773. https://doi.org/10.1016/j.jconrel.2020.10.010
64) Gupta, M. K., Martin, J. R., Werfel, T. A., Shen, T., Page, J. M., & Duvall, C. L. (2014). Cell protective, ABC triblock polymer-based thermoresponsive hydrogels with ROS-triggered degradation and drug release. *Journal of the American Chemical Society*, *136*(42), 14896–14902. https://doi.org/10.1021/ja507626y
65) Ford, C. A., Spoonmore, T. J., Gupta, M. K., Duvall, C. L., Guelcher, S. A., & Cassat, J. E. (2021). Diflunisal-loaded poly(propylene sulfide) nanoparticles decrease S. aureus-mediated bone destruction during osteomyelitis. *Journal of orthopaedic research : official publication of the Orthopaedic Research Society*, *39*(2), 426–437. https://doi.org/10.1002/jor.24948
66) Dollinger, B. R., Gupta, M. K., Martin, J. R., & Duvall, C. L. (2017). Reactive Oxygen Species Shielding Hydrogel for the Delivery of Adherent and Nonadherent Therapeutic Cell Types: *Tissue engineering. Part A*, *23*(19-20), 1120–1131. https://doi.org/10.1089/ten.tea.2016.0495
67) Liao, N., Shi, Y., Wang, Y., Liao, F., Zhao, B., Zheng, Y., Zeng, Y., Liu, X., & Liu, J. (2020). Antioxidant preconditioning improves therapeutic outcomes of adipose tissue-derived mesenchymal stem cells through enhancing intrahepatic engraftment efficiency in a mouse liver fibrosis model. *Stem cell research & therapy*, *11*(1), 237. https://doi.org/10.1186/s13287-020-01763-y
68) Friedenstein, A. J., Chailakhjan, R. K., & Lalykina, K. S. (1970). The development of fibroblast colonies in monolayer cultures of guinea-pig bone marrow and spleen cells. *Cell and tissue kinetics*, *3*(4), 393–403. https://doi.org/10.1111/j.1365-2184.1970.tb00347.x
69) Berebichez-Fridman, R., & Montero-Olvera, P. R. (2018). Sources and Clinical Applications of Mesenchymal Stem Cells: State-of-the-art review. *Sultan Qaboos University medical journal*, *18*(3), e264–e277. https://doi.org/10.18295/squmj.2018.18.03.002
70) Bhatti, F., Kim, S. J., Yi, A. K., Hasty, K. A., & Cho, H. (2018). Cytoprotective role of vitamin E in porcine adipose-tissue-derived mesenchymal stem cells against hydrogen-peroxide-induced oxidative stress. *Cell and tissue research*, *374*(1), 111–120. https://doi.org/10.1007/s00441-018-2857-3
71) Bernardo, M. E., & Fibbe, W. E. (2013). Mesenchymal stromal cells: sensors and switchers of inflammation. *Cell stem cell*, *13*(4), 392–402. https://doi.org/10.1016/j.stem.2013.09.006

72) Yang, J., Liao, X., Agarwal, M. K., Barnes, L., Auron, P. E., & Stark, G. R. (2007). Unphosphorylated STAT3 accumulates in response to IL-6 and activates transcription by binding to NFkappaB. *Genes & development*, *21*(11), 1396–1408. https://doi.org/10.1101/gad.1553707
73) Niada, S., Giannasi, C., Gomarasca, M., Stanco, D., Casati, S., & Brini, A. T. (2019). Adipose-derived stromal cell secretome reduces TNFα-induced hypertrophy and catabolic markers in primary human articular chondrocytes. *Stem cell research*, *38*, 101463. https://doi.org/10.1016/j.scr.2019.101463
74) Mei, L., Shen, B., Ling, P., Liu, S., Xue, J., Liu, F., Shao, H., Chen, J., Ma, A., & Liu, X. (2017). Culture-expanded allogenic adipose tissue-derived stem cells attenuate cartilage degeneration in an experimental rat osteoarthritis model. *PloS one*, *12*(4), e0176107. https://doi.org/10.1371/journal.pone.0176107
75) Jiang, L. B., Lee, S., Wang, Y., Xu, Q. T., Meng, D. H., & Zhang, J. (2016). Adipose-derived stem cells induce autophagic activation and inhibit catabolic response to pro-inflammatory cytokines in rat chondrocytes. *Osteoarthritis and cartilage*, *24*(6), 1071–1081. https://doi.org/10.1016/j.joca.2015.12.021
76) Bustin, S. A., Benes, V., Garson, J. A., Hellemans, J., Huggett, J., Kubista, M., Mueller, R., Nolan, T., Pfaffl, M. W., Shipley, G. L., Vandesompele, J., & Wittwer, C. T. (2009). The MIQE guidelines: minimum information for publication of quantitative real-time PCR experiments. *Clinical chemistry*, *55*(4), 611–622. https://doi.org/10.1373/clinchem.2008.112797
77) Cho, H., Seth, A., Warmbold, J., Robertson, J. T., & Hasty, K. A. (2011). Aging affects response to cyclic tensile stretch: paradigm for intervertebral disc degeneration. *European cells & materials*, *22*, 137–146. https://doi.org/10.22203/ecm.v022a11
78) Young, D. A., Barter, M. J., & Wilkinson, D. J. (2019). Recent advances in understanding the regulation of metalloproteinases. *F1000Research*, *8*, F1000 Faculty Rev-195. https://doi.org/10.12688/f1000research.17471.1
79) Raghu, H., Lepus, C. M., Wang, Q., Wong, H. H., Lingampalli, N., Oliviero, F., Punzi, L., Giori, N. J., Goodman, S. B., Chu, C. R., Sokolove, J. B., & Robinson, W. H. (2017). CCL2/CCR2, but not CCL5/CCR5, mediates monocyte recruitment, inflammation and cartilage destruction in osteoarthritis. *Annals of the rheumatic diseases*, *76*(5), 914–922. https://doi.org/10.1136/annrheumdis-2016-210426
80) Shen, J., Zhu, Y., Huang, K., Jiang, H., Shi, C., Xiong, X., Zhan, R., & Pan, J. (2016). Buyang Huanwu Decoction attenuates H2O2-induced apoptosis by inhibiting reactive oxygen species-mediated mitochondrial dysfunction pathway in human umbilical vein endothelial cells. *BMC complementary and alternative medicine*, *16*, 154. https://doi.org/10.1186/s12906-016-1152-7
81) Forman H. J. (2007). Use and abuse of exogenous H2O2 in studies of signal transduction. *Free radical biology & medicine*, *42*(7), 926–932. https://doi.org/10.1016/j.freeradbiomed.2007.01.011
82) Fink, S. L., & Cookson, B. T. (2005). Apoptosis, pyroptosis, and necrosis: mechanistic description of dead and dying eukaryotic cells. *Infection and immunity*, *73*(4), 1907–1916. https://doi.org/10.1128/IAI.73.4.1907-1916.2005

83) Das, R. H., Jahr, H., Verhaar, J. A., van der Linden, J. C., van Osch, G. J., & Weinans, H. (2008). In vitro expansion affects the response of chondrocytes to mechanical stimulation. *Osteoarthritis and cartilage, 16*(3), 385–391. https://doi.org/10.1016/j.joca.2007.07.014
84) Forsyth, C. B., Cole, A., Murphy, G., Bienias, J. L., Im, H. J., & Loeser, R. F., Jr (2005). Increased matrix metalloproteinase-13 production with aging by human articular chondrocytes in response to catabolic stimuli. *The journals of gerontology. Series A, Biological sciences and medical sciences, 60*(9), 1118–1124. https://doi.org/10.1093/gerona/60.9.1118
85) Arai, Y., Choi, B., Kim, B. J., Park, S., Park, H., Moon, J. J., & Lee, S. H. (2021). Cryptic ligand on collagen matrix unveiled by MMP13 accelerates bone tissue regeneration via MMP13/Integrin α3/RUNX2 feedback loop. *Acta biomaterialia*, S1742-7061(21)00137-9. Advance online publication. https://doi.org/10.1016/j.actbio.2021.02.042
86) Oh, S. J., Choi, K. U., Choi, S. W., Kim, S. D., Kong, S. K., Lee, S., & Cho, K. S. (2020). Comparative Analysis of Adipose-Derived Stromal Cells and Their Secretome for Auricular Cartilage Regeneration. *Stem cells international, 2020*, 8595940. https://doi.org/10.1155/2020/8595940
87) Zhang, R., Meng, F., Zhang, Q., Zou, Z., Xiao, K., Zhu, T., Li, H., Zhang, W., Ma, J., & Ma, J. (2021). Allogeneic adipose-derived mesenchymal stem cells promote the expression of chondrocyte redifferentiation markers and retard the progression of knee osteoarthritis in rabbits. *American journal of translational research, 13*(2), 632–645.